

## INFORMATION TO USERS

This manuscript has been reproduced from the microfilm master. UMI films the text directly from the original or copy submitted. Thus, some thesis and dissertation copies are in typewriter face, while others may be from any type of computer printer.

**The quality of this reproduction is dependent upon the quality of the copy submitted.** Broken or indistinct print, colored or poor quality illustrations and photographs, print bleedthrough, substandard margins, and improper alignment can adversely affect reproduction.

In the unlikely event that the author did not send UMI a complete manuscript and there are missing pages, these will be noted. Also, if unauthorized copyright material had to be removed, a note will indicate the deletion.

Oversize materials (e.g., maps, drawings, charts) are reproduced by sectioning the original, beginning at the upper left-hand corner and continuing from left to right in equal sections with small overlaps. Each original is also photographed in one exposure and is included in reduced form at the back of the book.

Photographs included in the original manuscript have been reproduced xerographically in this copy. Higher quality 6" x 9" black and white photographic prints are available for any photographs or illustrations appearing in this copy for an additional charge. Contact UMI directly to order.

# UMI

A Bell & Howell Information Company  
300 North Zeeb Road, Ann Arbor MI 48106-1346 USA  
313/761-4700 800/521-0600



**NMR STUDIES OF CYCLODEXTRIN INCLUSION  
COMPLEXES WITH NITROPHENOLS**

by

LIXUN YUAN

A dissertation submitted to the Graduate Faculty in  
Chemistry in partial fulfillment of the requirements for  
the degree of Doctor of Philosophy

The City University of New York.

1998

UMI Number: 9830782

Copyright 1998 by  
Yuan, Lixun

All rights reserved.

---

UMI Microform 9830782  
Copyright 1998, by UMI Company. All rights reserved.

This microform edition is protected against unauthorized  
copying under Title 17, United States Code.

---

**UMI**  
300 North Zeeb Road  
Ann Arbor, MI 48103

© 1998

LIXUN YUAN

ALL RIGHTS RESERVED

This manuscript has been read and accepted for the Graduate Faculty in Chemistry in satisfaction of the dissertation requirement for the degree of Doctor of Philosophy.

April 13, 1998

Date

Theresa Accardi

Chair of Examining Committee

April 28, 1998

Date

Gerold Kapp

Executive Officer

Theresa Accardi  
W. J. ...

V. Dot

Supervisory Committee

The City University of New York

## ABSTRACT

### NMR Studies of Cyclodextrin Inclusion Complexes with Nitrophenols

by

LIXUN YUAN

Advisor: Professor Theodore Axenrod

The inclusion complexes of  $\alpha$ -cyclodextrin ( $\alpha$ -CD) and permethylated  $\alpha$ -cyclodextrin ( $\alpha$ -MCD) with the two nitrophenols, 4-nitrophenol (4-NP) and 2,6-dimethyl-4-nitrophenol (2,6-DM-4-NP), were studied by means of  $^{15}\text{N}$ - $^1\text{H}$  heteronuclear Overhauser enhancement (NOE) experiments. Based on the enhancements of  $^{15}\text{N}$  resonances of the 4-nitrophenols upon irradiation at resonances of H-3 and H-5 inner protons in the cyclodextrin cavity, the results support the structures of these inclusion complexes. In these structures, the nitrophenols are preferentially inserted with the nitro group head first into the CD cavities and penetrated less deeply in the cavity of permethylated  $\alpha$ -CD than that of its parent cyclodextrin. Furthermore, these results are consistent with those derived from complexation-induced  $^1\text{H}$ ,  $^{13}\text{C}$  and  $^{15}\text{N}$  chemical shifts and NOESY experiments. The  $^{15}\text{N}$  spin-lattice relaxation time ( $T_1$ ) was determined for

the complexes of nitrophenols with  $\alpha$ - and  $\beta$ -cyclodextrins, and permethylated  $\alpha$ -cyclodextrin. The values obtained indicate that the complexes of  $\alpha$ -cyclodextrin with nitrophenols show weaker binding than the corresponding permethylated  $\alpha$ -cyclodextrin complexes and stronger binding than the corresponding  $\beta$ -cyclodextrin complexes. This observation supports the conclusion derived from the  $^{15}\text{N}$ - $^1\text{H}$  NOE experiments. The method of using  $^{15}\text{N}$ - $^1\text{H}$  nuclear Overhauser enhancement, while limited to guest molecules containing nitrogen, is shown to be useful when the dipolar interactions between protons involved in the cyclodextrin complex are too small to be measured. The advantage of using the  $^{15}\text{N}$ - $^1\text{H}$  NOE experiment is due to the large magnitude of the  $^{15}\text{N}$  resonance enhancement (maximum 400%), compared to that of the  $^1\text{H}$ - $^1\text{H}$  homonuclear NOE enhancement (maximum 50%).

## ACKNOWLEDGMENTS

I would like to specially thank my advisor, Dr. Theodore Axenrod, who generously advised me on a variety of academic issues as I was working on my Ph.D. degree. His special guidance and encouragement were always appreciated.

I also would like to thank the members of the thesis committee: Prof. V. G. S. Box and Prof. N. L. Yang for their valuable guidance and suggestions to make this thesis a success.

I am especially grateful to Dr. Clara Watnick for her friendship, many useful discussions and support in the writing of the thesis. It was a real pleasure to work with and learn from her.

I also would like to thank those teachers and friends who encouraged me to become a chemist and contributed to my educational achievements.

I am grateful to my parents and sisters for their love, encouragement, trust and support.

I am grateful to my wife for her exceptional devotion, support, patience and understanding which made the completion of this work possible.

# TABLE OF CONTENTS

	PAGE
<b>Abstract</b> .....	iv
<b>Acknowledgment</b> .....	vi
<b>Table of Contents</b> .....	vii
<b>List of Tables</b> .....	x
<b>List of Figures</b> .....	xi
<b>Chapter 1. Introduction</b>	
1.1 Scope .....	1
1.2 Cyclodextrins (CDs) and Their Inclusion Complexes .....	2
1.3 The Aspects of Spin-lattice Relaxation Times ( $T_1$ ) and Nuclear Overhauser Effect (NOE) .....	11
<b>Chapter 2. NMR Study of Nitrophenol Inclusion Complexes with Cyclodextrins</b>	
2.1 $^1\text{H}$ NMR Chemical Shift Measurements for the Inclusion Complexes of the $\alpha$ -Cyclodextrin and Permethylated $\alpha$ -Cyclodextrin with 4-Nitrophenols (4-NPs) .....	22
2.2 Cyclodextrin-induced Chemical Shift Changes in the	

	$^{13}\text{C}$ and $^{15}\text{N}$ NMR of 4-Nitrophenol (4-NP) .....	33
2.3	Determination of the Host-Guest Orientation in the Cyclodextrin (CD) Inclusion Complexes with 4-Nitrophenols (4-NPs) Using Homonuclear 2D NOE Spectroscopy (NOESY) .....	37
2.4	$^{15}\text{N}$ - $\{^1\text{H}\}$ Heteronuclear NOE as a Probe of Host-Guest Geometry in Cyclodextrin (CD) Inclusion Complexes with 4-Nitrophenols (4-NPs) .....	44
2.5	$^{15}\text{N}$ Spin-lattice Relaxation Time ( $T_1$ ) of Cyclodextrin (CD) Inclusion Complexes with 4-Nitrophenols (4-NPs) .....	58

### **Chapter 3. Experimental**

3.1	Materials .....	67
3.2	General Methods .....	67
3.3	Synthetic Methods .....	68
3.3.1	Synthesis of Permethyated- $\alpha$ -cyclodextrin ( $\alpha$ -MCD) .....	68
3.3.2	Synthesis of 4-Nitrophenol- $^{15}\text{N}$ (4-NP- $^{15}\text{N}$ ) .....	69
3.3.3	Synthesis of 2,6-Dimethyl-4-nitrophenol- $^{15}\text{N}$ (2,6-DM-4-NP- $^{15}\text{N}$ ) .....	72
3.4	NMR Methods .....	73
3.4.1	Sample preparation .....	73

3.4.2	NMR Spectroscopy .....	73
3.4.3	$^{15}\text{N}$ - $\{^1\text{H}\}$ Heteronuclear Overhauser Enhancement .....	74
3.4.4	Determination of $^{15}\text{N}$ Spin-lattice Relaxation Times .....	76
3.4.5	$^1\text{H}$ - $^1\text{H}$ COSY Experiments .....	76
3.4.6	NOESY Experiments .....	77
<b>Appendix A</b>	.....	<b>78</b>
<b>References</b>	.....	<b>89</b>

## LIST OF TABLES

	PAGE
<b>Table I.</b> Molecular Dimensions of Cyclodextrins .....	4
<b>Table II.</b> Dissociation Constants ( $K_d$ ) for $\alpha$ and $\beta$ -Cyclodextrin Inclusion Complexes with 4-NP in Aqueous Solution .....	21
<b>Table III.</b> Cyclodextrin Complexation-Induced $^{13}\text{C}$ and $^{15}\text{N}$ Chemical Shift Changes in 4-NP .....	34
<b>Table IV.</b> Heteronuclear $^{15}\text{N}$ - $\{^1\text{H}\}$ NOE Data from $\alpha$ -CD Complexes with 4-Nitrophenols- $^{15}\text{N}$ .....	45
<b>Table V.</b> Heteronuclear $^{15}\text{N}$ - $\{^1\text{H}\}$ NOE Data from $\alpha$ -MCD Complexes with 4-Nitrophenols- $^{15}\text{N}$ .....	55
<b>Table VI.</b> The NOE Enhancement with Different Irradiation Power .....	56
<b>Table VII.</b> $^{15}\text{N}$ Spin-lattice Relaxation Times ( $T_1$ ) of 4-NP and 2,6-DM-4-NP in Cyclodextrins Inclusion Complexes .....	59
<b>Table VIII.</b> Values of $^{15}\text{N}$ $T_1$ Ratios for the Free and Complexed 4-Nitrophenols with $\alpha$ - and $\beta$ -Cyclodextrins .....	60
<b>Table IX.</b> $^{15}\text{N}$ Spin-lattice Relaxation Times ( $T_1$ ) of 4-NP and 2,6-DM-4-NP in $\alpha$ -MCD inclusion complexes .....	62
<b>Table X.</b> Correlated $^1\text{H}$ , $^{13}\text{C}$ and $^{15}\text{N}$ Chemical Shifts (ppm)	

for $\alpha$ - and $\beta$ -Cyclodextrins and Their Corresponding Fully Nitrated Derivatives, Hexakis(2,3,6-tri- <i>O</i> -nitro)- $\alpha$ -cyclodextrin and Heptakis(2,3,6-tri- <i>O</i> -nitro)- $\beta$ -cyclodextrin, Measured in DMSO- <i>d</i> <sub>6</sub> .....	80
---	----

**Table XI.** Correlated <sup>1</sup>H, <sup>13</sup>C and <sup>15</sup>N Chemical Shifts (ppm)

Measured in DMSO- <i>d</i> <sub>6</sub> for Denitration Products, Hexakis(3,6-di- <i>O</i> -nitro)- $\alpha$ -cyclodextrin and Heptakis(3,6-di- <i>O</i> -nitro)- $\beta$ -cyclodextrin, Resulting from reactions of Hexakis(2,3,6-tri- <i>O</i> -nitro)- $\alpha$ -cyclodextrin and Heptakis(2,3,6-tri- <i>O</i> -nitro)- $\beta$ -cyclodextrin with Hydroxylamine in Pyridine .....	84
--	----

## LIST OF FIGURES

	PAGE
Figure 1. Molecular structure of $\beta$ -cyclodextrin .....	6
Figure 2. Two likely dispositions of 4-NP in cyclodextrin complexes .....	12
Figure 3. 300 MHz $^1\text{H}$ NMR spectra of $\alpha$ -CD alone and in the presence of 4-NP and 2,6-DM-4-NP at 1:3 molar ratio .....	23
Figure 4. 300 MHz $^1\text{H}$ COSY spectrum of $\alpha$ -CD complex with 4-NP .....	24
Figure 5. 300 MHz $^1\text{H}$ COSY spectrum of $\alpha$ -CD complex with 2,6-DM-4-NP .....	25
Figure 6. Comparison of the spectrum of $\alpha$ -MCD with the spectra of mixture of 4-NP and 2,6-DM-4-NP at 1:3 molar ratio each .....	28
Figure 7. 300 MHz $^1\text{H}$ COSY spectrum of $\alpha$ -MCD .....	29
Figure 8. 300 MHz $^1\text{H}$ COSY spectrum of $\alpha$ -MCD complex with 4-NP .....	30
Figure 9. 300 MHz $^1\text{H}$ COSY spectrum of the $\alpha$ -MCD complex with 2,6-DM-4-NP .....	31
Figure 10. The binding of an aromatic guest molecule	

	with $\alpha$ -CD is modeled by a biphasic field of two different dielectric constants .....	35
Figure 11.	300 MHz NOESY spectrum of $\alpha$ -CD inclusion complex with 2,6-DM-4-NP .....	40
Figure 12.	300 MHz NOESY spectrum of the $\alpha$ -MCD complex with 4-NP .....	41
Figure 13.	300 MHz NOESY spectrum of $\alpha$ -MCD complex with 2,6-DM-4-NP .....	42
Figure 14.	20 MHz heteronuclear $^{15}\text{N}$ - $\{^1\text{H}\}$ NOE difference spectra for the $\alpha$ -CD complex with 4-NP- $^{15}\text{N}$ .....	46
Figure 15.	20 MHz heteronuclear $^{15}\text{N}$ - $\{^1\text{H}\}$ NOE difference spectra for the $\alpha$ -CD complex with 2,6-DM-4-NP- $^{15}\text{N}$ .....	47
Figure 16.	Schematic representation of the host-guest orientation in the $\alpha$ -CD inclusion complexes with (top) 4-NP and (bottom) 2,6-DM-4-NP .....	48
Figure 17.	20 MHz heteronuclear $^{15}\text{N}$ - $\{^1\text{H}\}$ NOE difference spectra for the $\alpha$ -MCD complex with 4-NP- $^{15}\text{N}$ .....	52
Figure 18.	20 MHz heteronuclear $^{15}\text{N}$ - $\{^1\text{H}\}$ NOE difference spectra for the $\alpha$ -MCD complex with 2,6-DM-4-NP- $^{15}\text{N}$ .....	53

Figure 19. Schematic representation of the host-guest orientation in the $\alpha$ -MCD inclusion complexes with (top) 4-NP and (bottom) 2,6-DM-4-NP .....	54
Figure 20. IR spectra for $\alpha$ -CD (top) and $\alpha$ -MCD (bottom) measured in KBr pellet .....	70
Figure 21. 75 MHz $^{13}\text{C}$ spectrum of $\alpha$ -MCD in $\text{CDCl}_3$ .....	71
Figure 22. Contour plot of 300 MHz COSY 90 spectrum of heptakis(2,3,6-tri- <i>O</i> -nitro)- $\beta$ -cyclodextrin measured in $\text{DMSO-}d_6$ . .....	85
Figure 23. Contour plot of the $^{13}\text{C}$ - $^1\text{H}$ correlated spectrum of heptakis(2,3,6-tri- <i>O</i> -nitro)- $\beta$ -cyclodextrin measured in $\text{DMSO-}d_6$ . .....	86
Figure 24. Contour plot of the $^{15}\text{N}$ - $\text{O}$ - $\text{C}$ - $^1\text{H}$ correlated spectrum of heptakis(2,3,6-tri- <i>O</i> -nitro)- $\beta$ -cyclodextrin measured in $\text{DMSO-}d_6$ . .....	87
Figure 25. Comparison of 20 MHz $^{15}\text{N}$ spectra measured in $\text{DMSO-}d_6$ of (a) heptakis(2,3,6-tri- <i>O</i> -nitro)- $\beta$ -cyclodextrin- $^{15}\text{N}_{21}$ and (b) its denitration product, heptakis(3,6-di- <i>O</i> -nitro)- $\beta$ -cyclodextrin- $^{15}\text{N}_{14}$ , from reaction with hydroxylamine in pyridine. ....	88

# CHAPTER 1. INTRODUCTION

## 1.1 Scope

Since Demarco and Thakkar<sup>1</sup> presented direct evidence for the inclusion nature of the complex formation of  $\beta$ -cyclodextrin ( $\beta$ -CD) with aromatic guest molecules in aqueous solution by observing proton chemical-shift changes, NMR spectroscopy has been widely used for studies of cyclodextrin inclusion phenomena. With the introduction of superconducting higher-field magnets and modern computer systems, NMR has become indispensable for the study of cyclodextrin (CD) supramolecular chemistry in solution and in the solid state.<sup>2,3</sup>

The objective of this dissertation is to study the molecular structure and binding rigidity of CD inclusion complexes containing para-substituted nitrophenols as guest molecules using NMR methods. It is organized as follows: In Chapter 1, the structure, properties and uses of cyclodextrins (CDs) and their derivatives are discussed. An introduction to some theoretical considerations of spin-lattice relaxation time ( $T_1$ ) and nuclear Overhauser enhancement (NOE) is also presented. It provides a basis for the interpretation of the experimental results in subsequent chapters. In Chapter 2, the investigations of the host-guest geometry of CD inclusion complexes are described using complexation-induced  $^1\text{H}$ ,  $^{13}\text{C}$  and  $^{15}\text{N}$

chemical shifts.  $^1\text{H}$  homonuclear 2D NOE experiments and  $^{15}\text{N}\{-^1\text{H}\}$  heteronuclear NOE studies. The binding rigidity of the guest in CD cavity is estimated by  $^{15}\text{N}$  spin-lattice relaxation time experiments. Chapter 3 outlines the synthesis of required materials and presents the detailed experimental procedures.

## 1.2 Cyclodextrins (CDs) and Their Inclusion Complexes

Cyclodextrins (CDs) are water soluble compounds, first isolated in 1891 by Villiers<sup>4</sup> as degradation products of starch. In 1904, Schardinger<sup>5</sup> characterized them as cyclic oligosaccharides with a variable number of 1,4 linked  $\alpha$ -D-glucopyranose units. Cyclodextrins are obtained by treatment of starch with CD glucosyl transferases<sup>6</sup> which detach a turn from the starch helix and link the two ends of this fragment to produce a cyclic molecule. Since the enzymes never detach specific lengths uniformly, the resulting cyclodextrins contain 6 to 12 glucose units per ring.<sup>7</sup> The number of glucopyranose units is indicated by a Greek letter prefix, thus  $\alpha$ - for 6,  $\beta$ - for 7,  $\gamma$ - for 8,  $\delta$ - for 9, and so on.

The  $\alpha$ -,  $\beta$ - and  $\gamma$ -cyclodextrins ( $\alpha$ -,  $\beta$ - and  $\gamma$ -CDs),<sup>8</sup> the three major cyclodextrins, are crystalline and well characterized compounds. The relative quantities of these compounds in the fermentation mixture depends

on the type of enzyme employed. However, this distribution can be influenced by the addition of organic compounds.<sup>9</sup>

Based on conformational energy map calculations, Sundararajan and Rao<sup>10</sup> suggested that cyclodextrins with less than six ring members cannot be formed for steric reasons. However, Nakagawa, Ueno, Kashiwa and Watanabe<sup>11</sup> reported the chemical synthesis of a five-membered CD, which has been characterized by fast-atom bombardment mass spectrometry (FABMS).

In addition to the major cyclodextrins described above, there are several papers in the CD literature describing the minor cyclodextrins with 9, 10, 11 and 12 glucose units. The nine-membered  $\delta$ -CD was isolated from the commercially available CD mixture by chromatography; however, this was not characterized unambiguously.<sup>8</sup> The 12-membered  $\eta$ -CD was also isolated from the CD mixture by chromatography. Its molecular weight was found to be 1946.6 Da by FABMS and its structure was verified by <sup>13</sup>C NMR spectroscopy.<sup>12</sup> French, Pulley, Efenburger, Abdullar and Rougvié<sup>6,7</sup> reported the 10- and 11-membered ring cyclodextrins, but their characterization was inconclusive.

For the major cyclodextrins, the CD molecule is a truncated cone<sup>13,14,15</sup> with the primary and secondary hydroxyl groups located on the narrower and the wider rims, respectively. As a result of this arrangement,

**Table I. Molecular Dimensions of Cyclodextrins<sup>8</sup>**

cyclodextrin	glucose units	cavity dimension (Å)	
		diameter	depth
$\alpha$ -CD	6	~ 4.9	~ 7.9
$\beta$ -CD	7	~ 6.2	~ 7.9
$\gamma$ -CD	8	~ 7.9	~ 7.9

the external faces of CDs are hydrophilic. The methine protons, H-3 and H-5, and the glycosidic oxygen bridges are oriented in its interior. Therefore the space inside the cone, called the cavity, is relatively hydrophobic. In the cyclodextrin molecules, a ring of hydrogen bonds is formed between the 2-hydroxyl and 3-hydroxyl groups of adjacent glucose units. This hydrogen bonding ring gives the cyclodextrin a rigid structure. The above structural features are illustrated in Figure 1 for  $\beta$ -CD. The internal CD cavity diameter varies according to the number of glucose residues present and the dimensions as measured by X-ray diffraction<sup>16</sup> are summarized in Table I.

The  $\alpha$ -,  $\beta$ - and  $\gamma$ -CDs with water solubilities of 14.5, 1.85 and 23.2 g/100 mL, respectively,<sup>2</sup> are used extensively as solubilizing transport agents. The degree of solubility of the CD is related to their structural features.  $\beta$ -CD is a rather rigid structure<sup>17</sup> because a complete secondary belt is formed by hydrogen bonds between 2- and 3-hydroxyl groups of adjacent glucose units. This structure probably explains the observation that  $\beta$ -CD has the lowest solubility of cyclodextrins. The hydrogen bond belt is incomplete in the  $\alpha$ -CD molecule because one glucopyranose unit is in a distorted position.<sup>18,19</sup> Consequently, instead of the six possible hydrogen bonds, only four can be established. The  $\gamma$ -CD molecule has a more flexible structure, and is therefore the most soluble of the three CDs.

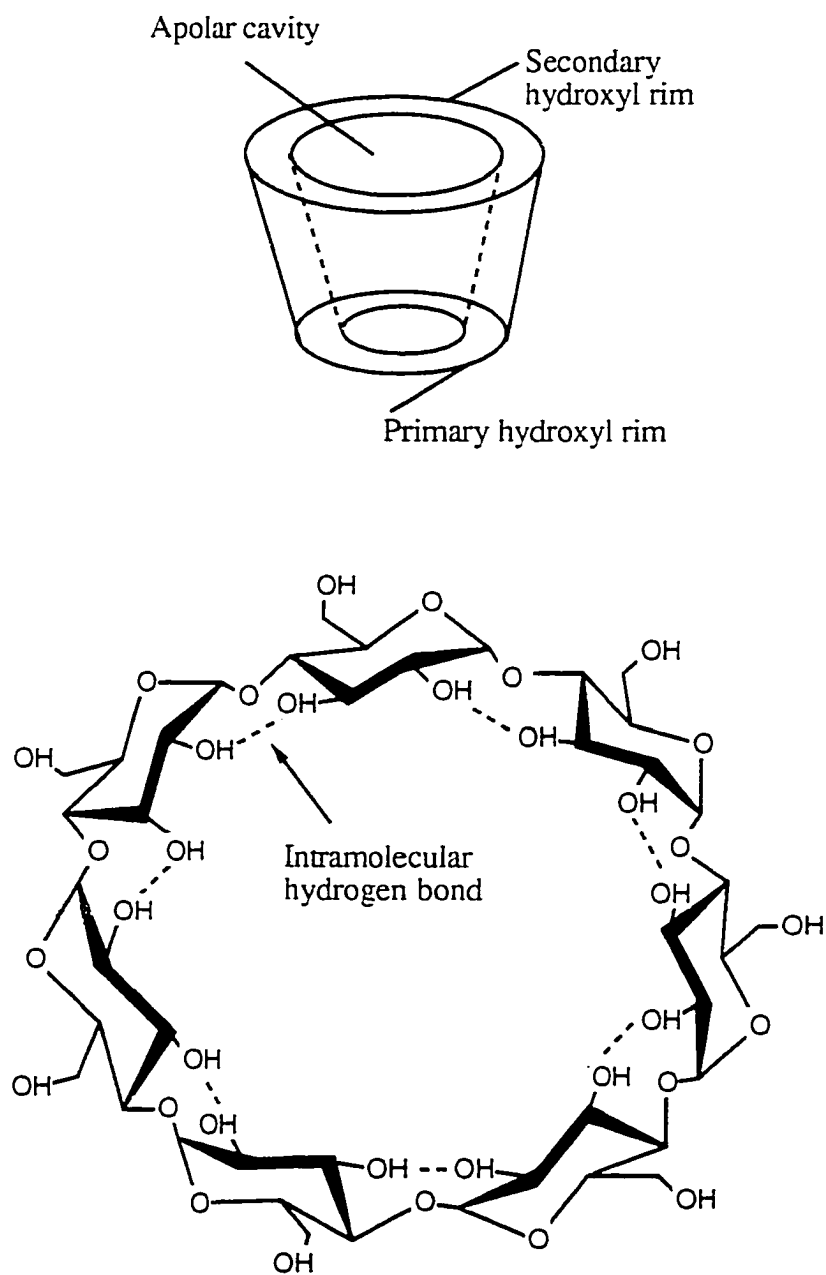


**Figure 1.** Molecular structure of  $\beta$ -cyclodextrin.

The most characteristic property of cyclodextrins is their ability to encapsulate a large variety of molecules ranging from neutral or ionic organic and inorganic compounds to noble gases.<sup>15</sup> This molecular complexation confers on the guest molecule new physicochemical properties of great value for many different applications. Complexation with cyclodextrins, for example, is used for the solubility enhancement of water insoluble drugs,<sup>20,21</sup> encapsulation and removal of environmental pollutants,<sup>22</sup> and protection of certain foods and food additives against oxidation, light and heat.<sup>23</sup>

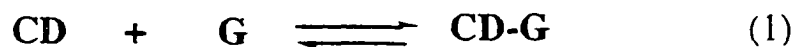
Recently, various kinds of cyclodextrin derivatives have been prepared to modify the physicochemical properties and extend the inclusion capacity of natural cyclodextrins. Generally, the chemically modified cyclodextrins can be divided into three groups:<sup>24,25</sup> (1) hydrophilic, (2) hydrophobic and (3) ionizable derivatives.<sup>26</sup> The hydrophilic derivatives in the first group, such as methylated cyclodextrins,<sup>27</sup> hydroxypropyl cyclodextrin<sup>28</sup> and branched cyclodextrins,<sup>29</sup> deserve special attention since their solubility in water is very high. This is a desirable property when using these CDs for the transport of poorly water-soluble guests. The hydrophobic cyclodextrins in the second group, such as alkylated cyclodextrins, which have the ability to decrease the solubility of guest molecules, are useful as sustained-release drug carriers of water-soluble drugs.<sup>30</sup> The ionizable cyclodextrins in the third group, such as carboxy

ethyl cyclodextrin, can modify the rate of release of guest molecules, depending on the pH value of the solution and binding constants of the complexes.<sup>26</sup>

The methylated cyclodextrins are among the first water-soluble derivatives described in the literature.<sup>2</sup> Partial and full methylation of cyclodextrins can enhance their solubility in aqueous solution enabling them to form inclusion complexes,<sup>2</sup> some of which are more stable than those of their parent cyclodextrins. The change in physical and complexation properties of methylated cyclodextrins can be explained if one assumes that the shape of the macrocyclic ring changes when hydrogen bonding between the secondary hydroxyl groups is prevented. The methylation of the hydroxyl groups is expected to increase the extent of the apolar sphere of the CD cavity. Consequently, methylation may result in an increase of the binding tendency of the apolar guest molecule to the cyclodextrin cavity. For example, for permethylated  $\alpha$ -CD ( $\alpha$ -MCD), one of the most simple derivatives, the dissociation constant for complexation with 4-nitrophenol (4-NP) in alkaline solution determined by  $^1\text{H}$  NMR is  $8.0 \times 10^{-5} \text{ M}$ , while that for  $\alpha$ -CD complex is  $6.1 \times 10^{-4} \text{ M}$ ,<sup>31</sup> one order of magnitude smaller as expected for the proposed model.

Complexation in solution is a dynamic equilibrium process.<sup>32</sup> The formation of a 1:1 inclusion complex is illustrated by equation 1, where

CD, G and CD-G are cyclodextrin, guest molecule and cyclodextrin-guest complex, respectively. The binding forces responsible for substrate binding



can be quantitatively described by a complexation constant (  $K_c$  ) or its reciprocal dissociation constant (  $K_d$  ) as defined in equation 2.

$$K_c = \frac{1}{K_d} = \frac{[\text{CD-G}]}{[\text{CD}][\text{G}]} \quad (2)$$

Although numerous papers have been published on the elucidation of the mechanism leading to the formation of CD inclusion complexes, the precise nature of the binding forces involved in complexation is not fully understood.<sup>3</sup> However, it is widely accepted that the stabilities of CD inclusion complexes are governed by several factors which include hydrogen bonding, hydrophobic interactions, dispersive interactions, dipolar interactions, release of distortional energy and extrusion of high energy water from the CD upon inclusion of guest, the polarity of the guest molecule, and the guest molecular size and shape<sup>33,34</sup> Since a good match between the guest size and that of the CD cavity is essential for efficient

intermolecular contacts, the size of the guest is among the more important factors in determining the stability of the CD complex.

In order to understand the formation mechanism of CD inclusion complexes, the spatial structures of inclusion complexes and the various interactions contributing to their formation must be well characterized. NMR parameters such as chemical shift, spin coupling constant, nuclear Overhauser enhancement (NOE), and relaxation time are sensitive to intermolecular interactions. A consideration of the structural possibilities for the  $\alpha$ -CD complex with 4-nitrophenol (4-NP) suggests that 4-NP can only penetrate the CD cavity effectively in one of two different orientations, either the hydroxyl group or the nitro group end first as shown in Figure 2.<sup>35</sup> A third orientation penetrating through the *ortho* and *meta* positions is unreasonable, because very little of the substrate would fit into the cavity. Bergeron<sup>35</sup> distinguished between these possibilities by <sup>1</sup>H NMR and NOE. He found that the *meta* proton resonance of 4-NP was shifted substantially more than the *ortho* proton resonance, and that after irradiation of the H-5 protons of  $\alpha$ -CD there was a greater signal enhancement for the *meta* protons compared to the *ortho* protons, indicating that the nitro group head penetrates the  $\alpha$ -CD cavity first.

### 1.3 The Aspects of Spin-lattice Relaxation Time ( $T_1$ ) and Nuclear Overhauser Effect (NOE)

Relaxation, the central phenomenon of nuclear magnetic resonance, has received considerable attention from both theoreticians and experimentalists,<sup>36</sup> because relaxation experiments can be used to probe molecular structure and molecular motion.

The process of spin-lattice relaxation is an energy exchange between nuclear spins and the lattice resulting in the establishment of equilibrium between populations in the nuclear spin energy levels. The spin-lattice relaxation time ( $T_1$ ) values are affected by the media and molecular structural features,<sup>37</sup> occurring in solution.

Spin-lattice relaxation is dominated by one of five mechanisms:<sup>38</sup> (1) **dipole-dipole interactions:** Such dipolar interactions are the most important way in which the motions of the molecule produce the randomly varying local field to induce relaxation. (2) **quadrupolar relaxation:** This is normally the dominant relaxation mechanism for nuclei with quantum number  $I > 1/2$ , such as  $^2\text{H}$  and  $^{14}\text{N}$ . These nuclei, in addition to being dipolar, are also quadrupolar. (3) **chemical shift anisotropy (CSA) relaxation:** All bonds are anisotropic, and consequently produce a different field at a nucleus depending on the orientation of the bond

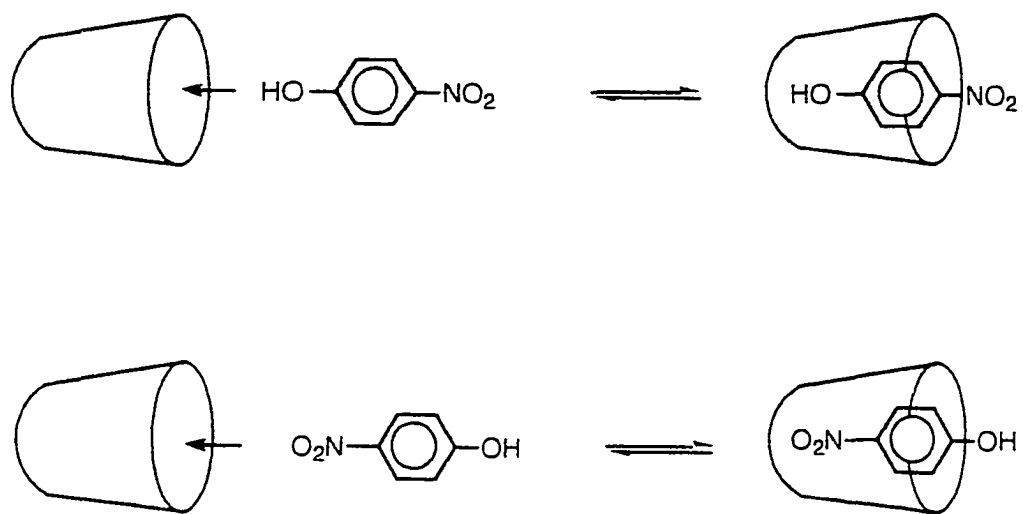


**Figure 2.** Two likely dispositions of 4-NP in cyclodextrin complexes.

relative to the applied field. (4) **scalar relaxation**: Scalar, or spin-spin coupling refers to one of the local field which depends on the spin state of its coupling partner, and vice versa. (5) **spin-rotation relaxation**: Spin-rotation relaxation occurs when a molecule, or a group of atoms within a molecule, undergoes transitions between one rotational state and another.

It is well-known that the  $T_1$  value for any given molecule in solution depends upon molecular mobility (tumbling) and specific internal motions as determined by the degrees of freedom in the molecule.<sup>38,39</sup> In a series of cyclodextrin complexes, a comparison of  $T_1$  values for the same nucleus in each of the complexes could give information about the relative stabilities of the inclusion complexes. That is, the relative magnitude of the  $T_1$  values is an indication of the tightness with which the substrate fits into the cavity and the mobility it has to rotate or move within the cavity of the cyclodextrin. Compounds with large molecular weights or molecular volume tumble more slowly than smaller molecules, and thus exhibit shorter relaxation times than the smaller systems. Inclusion complexation results in an increase in the effective molecular volume. Consequently, there is less freedom for the inclusion complex to tumble resulting in a decrease in  $T_1$  or an increase in correlation time  $\tau_c$  which is the average time taken to rotate through one radian or roughly the reciprocal of the rate of tumbling in solution of the relevant piece of the molecule. As we assume that the spin-lattice relaxation rates of nuclei in these inclusion

complexes are dominated by dipolar relaxation between the nucleus in the substrate and the protons inside the cyclodextrin cavity, the rate of dipolar relaxation ( $\mathbf{R}$ ) is directly proportional to the correlation time  $\tau_c$  and governed by a strong  $r^{-6}$  dependence between these nuclei where  $r$  is the internuclear distance.<sup>3</sup> The changes in distance between the nucleus in the

$$\mathbf{R} \sim \tau_c / r^6 \quad (3)$$

substrate and protons in the cyclodextrin cavity by complexation will result in a change of the relaxation rate.

In the limit of the rapid exchange process of equation 1, a weighted average relaxation rate,  $1/T_1$ , given by equation 4, is measured. Here  $1/T_{1f}$  and  $1/T_{1c}$  are the spin-lattice relaxation rate for a spin in the free

$$1/T_1 \rightleftharpoons P_f (1/T_{1f}) + P_c (1/T_{1c}) \quad (4)$$

and complexed states, and  $P_f$  and  $P_c$  are the probabilities that  $G$  is found in the free and in the complexed states. The values of  $P_c$  and  $P_f$  can be determined from the association constant.

Fundamentals of the theory of the Nuclear Overhauser Effect (NOE) were established in 1955 by Solomon.<sup>40</sup> Since that time an increasing number of chemical applications have appeared in the literature.

Studies of spin-lattice relaxation<sup>41</sup> and NOE<sup>42,43</sup> have proved to be direct and powerful methods of structure elucidation. The study of multi-spin dipolar relaxation not only provides geometric information, but also gives a deeper insight into molecular reorientational processes.

Most of the chemical applications of the NOE are based on its inverse sixth power dependence on intermolecular distance, which allows the homo- and heteronuclear experiments to be used for structural determination of molecules in the liquid phase. In addition to the qualitative structural information obtained by demonstrating the proximity of two nuclei in space, steady-state heteronuclear NOE measurements also allow one to determine the internuclear distances.<sup>44,45</sup>

In theory,<sup>46</sup> NOE and relaxation rate are treated together because their origins, measurement, and interpretation are entwined. In the NMR experiment, excess spin population moved from one energy level to another by electromagnetic radiation of the appropriate frequency is called excitation. The radiationless return to equilibrium is called spin-lattice relaxation because the excess energy passes from the spin to the lattice as heat. This relaxation requires magnetic fields that are fluctuating at the irradiated frequency. The rate of dipole-dipole relaxation depends on the strength and frequency of the fluctuating magnetic fields. These, in turn, depend on three factors: (1) the distance between the nuclei involved; (2) the effective correlation time,  $\tau_c$ ; and (3) the nature of the nuclei

themselves. NOE and the relaxation rate are also measures of the strength of the dipole-dipole interaction between the nuclei and are dependent on interatomic distances.

## CHAPTER 2. NMR STUDY OF NITROPHENOL INCLUSION COMPLEXES WITH CYCLODEXTRINS

The extent to which 4-nitrophenol penetrates the  $\alpha$ -cyclodextrin cavity has been defined by the Cross-polarization magic-angle sample spinning (CPMAS)  $^{13}\text{C}$  NMR studies of the complexes in solid state by Inoue, Kuan, Takahashi and Chujo<sup>47</sup> and in aqueous solution using  $^1\text{H}$  NMR by Bergeron and Rowar.<sup>35</sup> In both the solid state and in solution, the 4-nitrophenyl group is located in the host cavity and the OH group protrudes from the secondary hydroxyl side of the CD cavity. In solution, additional support for this structure comes from intermolecular 1D  $^1\text{H}$ - $\{^1\text{H}\}$  NOE data given by Inoue, Takahashi and Chujo.<sup>31</sup> In 1D NOE, a substantial enhancement of the resonances of H-3' and H-2' protons (*meta* and *ortho* to the phenolic hydroxyl-group, respectively) of 4-nitrophenol was observed upon selective irradiation at the resonance frequency of the H-3 signal of  $\alpha$ -CD while irradiation at the resonance frequency of the H-5 signal enhanced the H-3' proton resonance only. These results support a structure in which the 4-NP is preferentially inserted with the nitro group head first into the  $\alpha$ -CD cavity. Further confirmation for this orientation is obtained from 2D  $^1\text{H}$ - $^1\text{H}$  NOE data given by Inoue, Yamamoto, Onda and Kitagawa.<sup>48</sup> The 2D NOE data show cross peaks connect the H-3 resonance of the  $\alpha$ -CD to both H-3' and H-2' protons of 4-NP but connect H-5 to only

the H-3' proton. The  $^{13}\text{C}$  NMR studies of the  $\alpha$ -CD inclusion complex with 4-NP in aqueous solution described by Inoue, Hoshi, Sakurai and Chujo<sup>49</sup> also show that the phenyl C-4' is extensively shielded in contrast to the deshielding of corresponding C-1'. On this basis, the guest is inserted into the  $\alpha$ -CD cavity with the nitro substituent in the lead. These characteristic  $^{13}\text{C}$  displacements induced by complexation with  $\alpha$ -CD are also useful in the determination of the orientation of the guest in the  $\alpha$ -CD cavity.

Based on the NMR data obtained, Bergeron and Channing<sup>50,51</sup> assigned to the 2,6-DM-4-NP- $\alpha$ -CD complex a structure similar to that of the 4-NP- $\alpha$ -CD complex. Their conclusion was based on the 22% NOE enhancement obtained for the H-3' signal of the 2,6-DM-4-NP after irradiation of the  $\alpha$ -CD cavity protons. However, this non-selective irradiation of the  $\alpha$ -CD cavity protons gives no information on the extent of penetration of the 2,6-DM-4-NP molecule.

The X-ray crystallographic studies of  $\alpha$ -MCD<sup>52</sup> show that the size of the secondary hydroxyl side of the cyclodextrin cavity is widened and the primary hydroxyl side is narrowed by the methylation of all hydroxyl groups due to the absence of hydrogen bonding between the secondary hydroxyl groups as well as the repulsive interaction of adjacent methoxyl groups. Botsi, Yannakopoulou, Hadjoudis and Perly<sup>53</sup> confirmed that the structure of the  $\alpha$ -MCD in solution resembles that of solid state.

The host-guest interaction in the  $\alpha$ -MCD-4-NP complex in the solid state is quite different from that found in the  $\alpha$ -CD-4-NP complex<sup>51</sup> in which the nitrophenyl group is tightly bound in the  $\alpha$ -CD cavity, while the hydroxyl group protrudes from the secondary hydroxyl side of the cavity. An upside-down inclusion has been observed in the  $\alpha$ -MCD-4-NP complex<sup>52</sup> in which the hydroxyl group of the 4-NP is inserted into the  $\alpha$ -MCD-4-NP ring. Harata, Uekama, Otagiri and Hirayama<sup>52</sup> attributed such a change in the inclusion geometry to the difference in the shape and size of the host cavity. The  $\alpha$ -CD cavity is quite suitable to accommodate the nitrophenyl group, but the methylation of all hydroxyl groups of  $\alpha$ -CD makes the primary hydroxyl side so narrow that the nitrophenyl group can not be deeply inserted. In this case, the choice of the substitute group to be included seems to depend upon the steric hindrance.<sup>52</sup>

Inoue, Takahashi and Chujo<sup>31</sup> suggested that in aqueous solution the position of 4-NP in the  $\alpha$ -MCD cavity, defined by the <sup>1</sup>H NMR spectra, resembles that found in the  $\alpha$ -CD cavity since clear down-field shifts are induced for both resonances of H-3' and H-2' protons of 4-NP by  $\alpha$ -CD as well as by  $\alpha$ -MCD.<sup>31</sup> They tried to clarify the orientation of the 4-NP in  $\alpha$ -MCD cavity. However, the <sup>1</sup>H-<sup>1</sup>H NOE for the  $\alpha$ -MCD-4-NP system could not be observed, probably owing to the weak dipolar interaction between the 4-nitrophenol protons and the inner protons of the  $\alpha$ -MCD. Furthermore, because in solution the guest molecule included in the CD

cavity is not at rest, but is in fairly rapid motion, it is not easy to observe  $^1\text{H}$ - $^1\text{H}$  NOE enhancement.<sup>3</sup> We therefore present a confirmation of the orientation of 4-nitrophenols in  $\alpha$ -MCD cavity using  $^{15}\text{N}$  NMR experiments.

From the  $^1\text{H}$  and  $^{13}\text{C}$  NMR data obtained above, it is expected that a comparable degree of heteronuclear intermolecular dipolar relaxation inside the CD cavity may exist between the  $^{15}\text{N}$  atom in 4-nitrophenols and the H-3 and H-5 CD protons, especially the H-5 protons. In the present work, the extent of this heteronuclear interaction is studied by measuring the  $^{15}\text{N}$  chemical shift,  $^{15}\text{N}$  spin-lattice relaxation time and  $^{15}\text{N}$ - $\{^1\text{H}\}$  heteronuclear NOE experiments to obtain information regarding the geometry and binding rigidity of 4-nitrophenol inclusion complexes with  $\alpha$ -cyclodextrin and permethylated  $\alpha$ -cyclodextrin.

In  $^{15}\text{N}$  NMR spectroscopy,<sup>55</sup> the detection of  $^{15}\text{N}$  resonances is more difficult due to its inherent lower natural abundance as well as due to its  $T_1$  values being several orders of magnitude longer than that of  $^{13}\text{C}$  resonance. Furthermore, the NOE, advantageous for  $^{13}\text{C}$  NMR spectroscopy, can be a detriment for  $^{15}\text{N}$  owing to its negative gyromagnetic ratio. To minimize the problems of the signal/noise ratio, 99% enriched 4-NP- $^{15}\text{N}$  and 2,6-DM-4-NP- $^{15}\text{N}$  were used. On the other hand, a maximum NOE, arising from the exclusive dipole-dipole relaxation, gives rise to an inverted signal

**Table II Dissociation Constants ( $K_d$ )<sup>a</sup> for  $\alpha$ - and  $\beta$ -Cyclodextrin Inclusion Complexes with 4-NP in Aqueous Solution<sup>56</sup>**

	pD 6	pD 10
$\alpha$ -CD	$2.5 \times 10^{-3}$	$6.1 \times 10^{-4}$
$\beta$ -CD	$3.9 \times 10^{-3}$	$1.5 \times 10^{-3}$

<sup>a</sup>Dissociation constants are given in M and determined by <sup>1</sup>H NMR.

with an intensity enhanced by a factor of four, with which a large sensitivity may be obtained for the  $^{15}\text{N}\text{-}\{^1\text{H}\}$  NOE determination.

In addition, cyclodextrins are known to have stronger affinities for organic anions than for neutral forms. For example, the dissociation constants of  $\alpha$ -CD and  $\beta$ -CD with the 4-NP ion in alkaline aqueous solution are considerably smaller than those of their neutral forms,<sup>56</sup> as shown in Table II. Accordingly, the heteronuclear NOE experiments were carried out at a pD of 11 in a phosphate buffer solution. Furthermore, the solubilities of the complexes are greater in alkaline solution, which is a particularly important consideration in the case of the sparingly soluble  $\beta$ -cyclodextrin.

## 2.1 $^1\text{H}$ NMR Chemical Shift Measurements for the Inclusion Complexes of $\alpha$ -Cyclodextrin ( $\alpha$ -CD) and Permethylated $\alpha$ -Cyclodextrin ( $\alpha$ -MCD) with 4-Nitrophenols (4-NPs)

The  $^1\text{H}$  NMR spectra of  $\alpha$ -cyclodextrin in the absence and presence of either 4-nitrophenol (4-NP) or 2,6-dimethyl-4-nitrophenol (2,6-DM-4-NP) in an alkaline buffer solution (pD 11) are illustrated in Figure 3. The proton assignments for the  $\alpha$ -CD-4-NP and  $\alpha$ -CD-2,6-DM-4-NP inclusion complexes are based on  $^1\text{H}\text{-}^1\text{H}$  correlation 2D NMR experiments (COSY) as shown in Figures 4 and 5, respectively. The resonances of H-1 in the

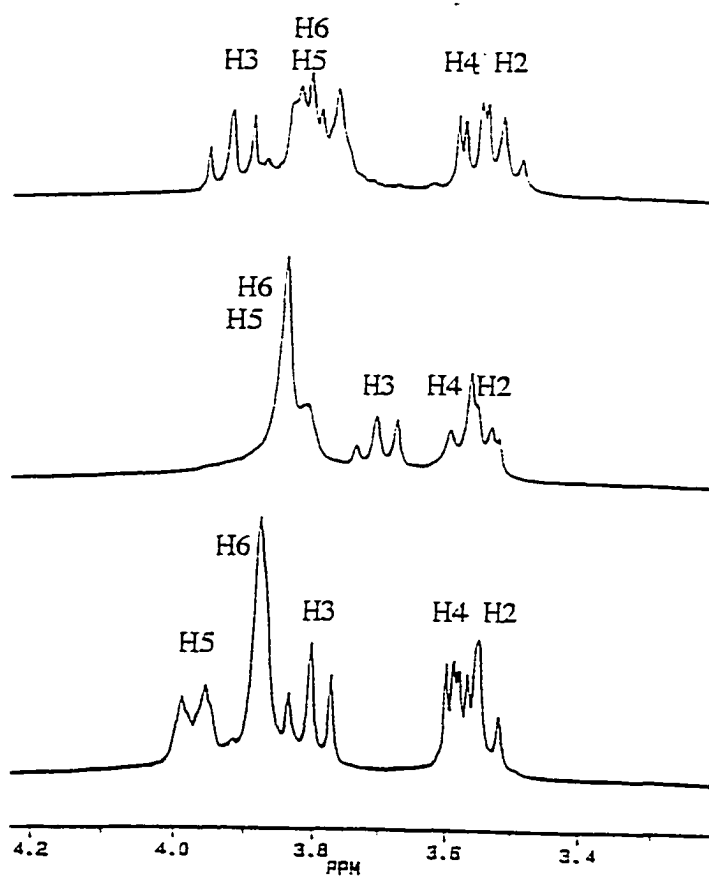


**Figure 3.** 300 MHz  $^1\text{H}$  NMR spectra of  $\alpha$ -CD (top) alone and in the presence of 4-NP (middle), and 2,6-DM-4-NP (bottom) at 1:3 molar ratio.

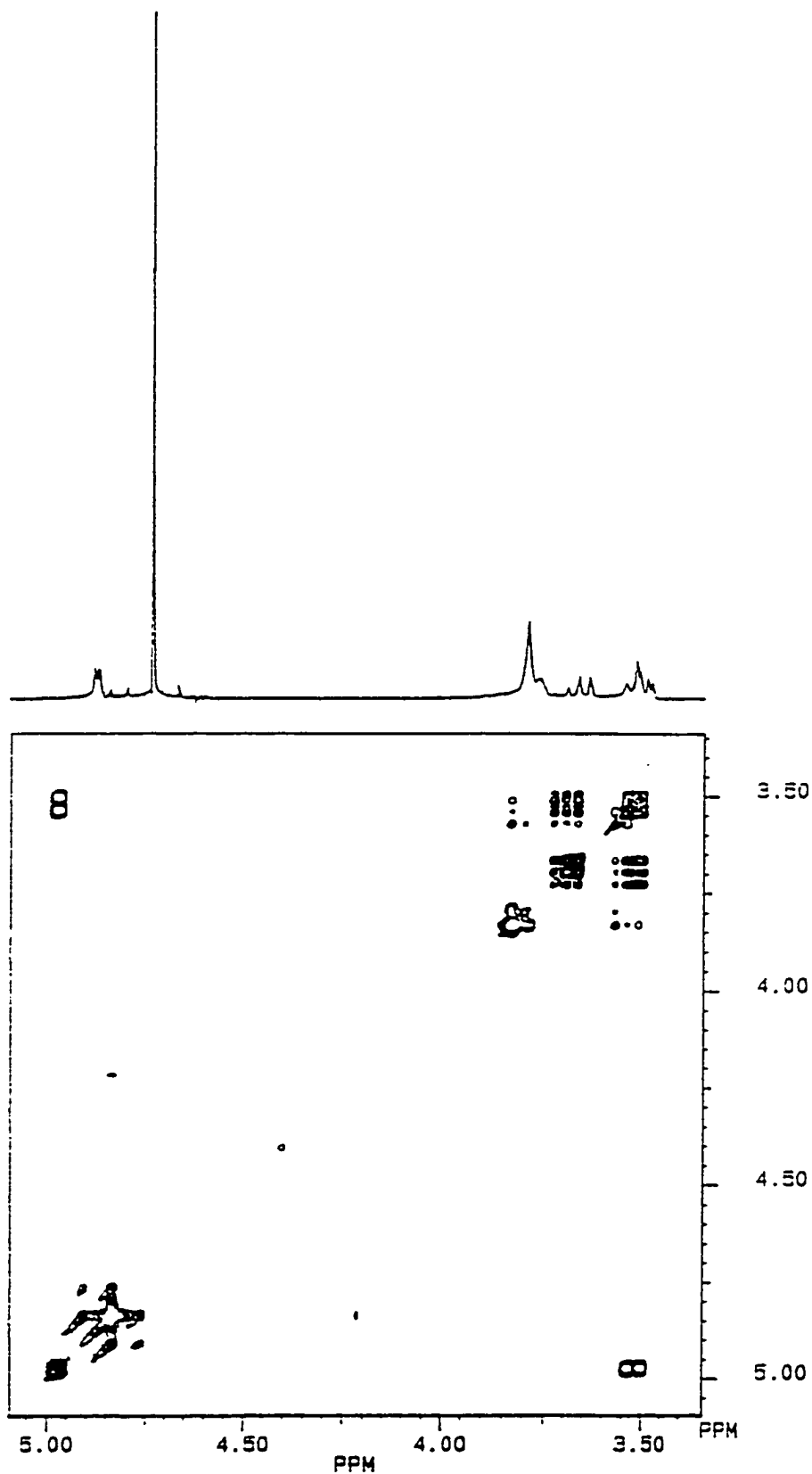


**Figure 4.** 300 MHz  $^1\text{H}$  COSY spectrum of  $\alpha$ -CD complex with 4-NP.



**Figure 5.** 300 MHz  $^1\text{H}$  COSY spectrum of  $\alpha$ -CD complex with 2,6-DM-4-NP.

cyclodextrin display a considerable down-field shift compared with those of other methine protons in cyclodextrin. Beginning on the diagonal with the resonances for H-1, the resonances for H-2 may be located by connecting the cross peaks with H-1, and so on for the other ring protons.

The  $^1\text{H}$  NMR spectra of  $\alpha$ -CD complexes with 4-NP and 2,6-DM-4-NP show significant upfield shifts of H-3, whereas the frequency of H-5 is not altered for the 4-NP complex and undergoes large downfield shift for 2,6-DM-4-NP complex. The 2,6-DM-4-NP induced shifts in the CD cavity are similar, although not identical to those in the 4-NP complex.<sup>50</sup> The H-3 shielding is certainly due to the ring-current effect of the included nitrophenols, the H-5 deshielding for 2,6-DM-4-NP complex may be that the 2,6-methyl groups of the substrate help to hold the nitro oxygens in intimate contact with the H-5 protons of  $\alpha$ -CD resulting in charge deshielding. Bergeron, Channing, Gibeily and Pillor<sup>50</sup> suggest that introduction of methyl groups at the 2 and 6 position in the 4-NP limits the depth of substrate penetration to the cavity.

Botsi, Yannakopoulou, Hdjoudis and Perly.<sup>53</sup> determined the  $^1\text{H}$  and  $^{13}\text{C}$  assignments for  $\alpha$ -MCD in  $\text{D}_2\text{O}$  using homo and hetero 2D NMR experiments. However, the literature  $^1\text{H}$  spectra of  $\alpha$ -MCD in  $\text{D}_2\text{O}$  could not always be used as reference, and that the reported assignments should be treated with caution owing to the dependence of the positions of the NMR signals on the conditions used, such as internal standards, pH,

concentration and temperature. In this work, the  $^1\text{H}$  assignments for  $\alpha$ -MCD in the absence and presence of 4-NP and 2,6-DM-4-NP in an alkaline buffer solution (pD11) are completed based on 2D  $^1\text{H}$  chemical shift correlation spectroscopy (COSY) experiments. The  $^1\text{H}$  NMR spectra of  $\alpha$ -MCD and its complexes in an alkaline buffer solution (pD 11) are shown in Figure 6. The COSY spectra are illustrated in Figures 7, 8 and 9, respectively. The 300 MHz spectra for these inclusion complexes recorded in Figure 6 show that the H-3 resonances are hidden under the  $\text{CH}_3\text{O}$ -6 resonances, their exact positions, however, are confirmed by the cross peaks from COSY experiments.

The 4-nitrophenols induce upfield-shifting for all  $\alpha$ -MCD protons with the exception of H-5, the chemical shift changes for H-3, however, are much more substantial due to the anisotropic shielding effects arising from the aromatic ring of the phenolic group. Likewise, the proton resonances of the secondary methoxyl groups,  $\text{CH}_3\text{O}$ -2 and  $\text{CH}_3\text{O}$ -3, move significantly upfield. By contrast, H-5 resonances experience downfield-shifting probably due to the charge deshielding from the nitro oxygens of the substrates to the H-5 protons of the  $\alpha$ -MCD as described for the 2,6-DM-4-NP- $\alpha$ -CD complex.<sup>35</sup> These observations demonstrate that in the  $\alpha$ -MCD complexes the 4-nitrophenols enter into the  $\alpha$ -MCD cavity from the secondary methoxyl side. The fact that all CD protons undergo chemical

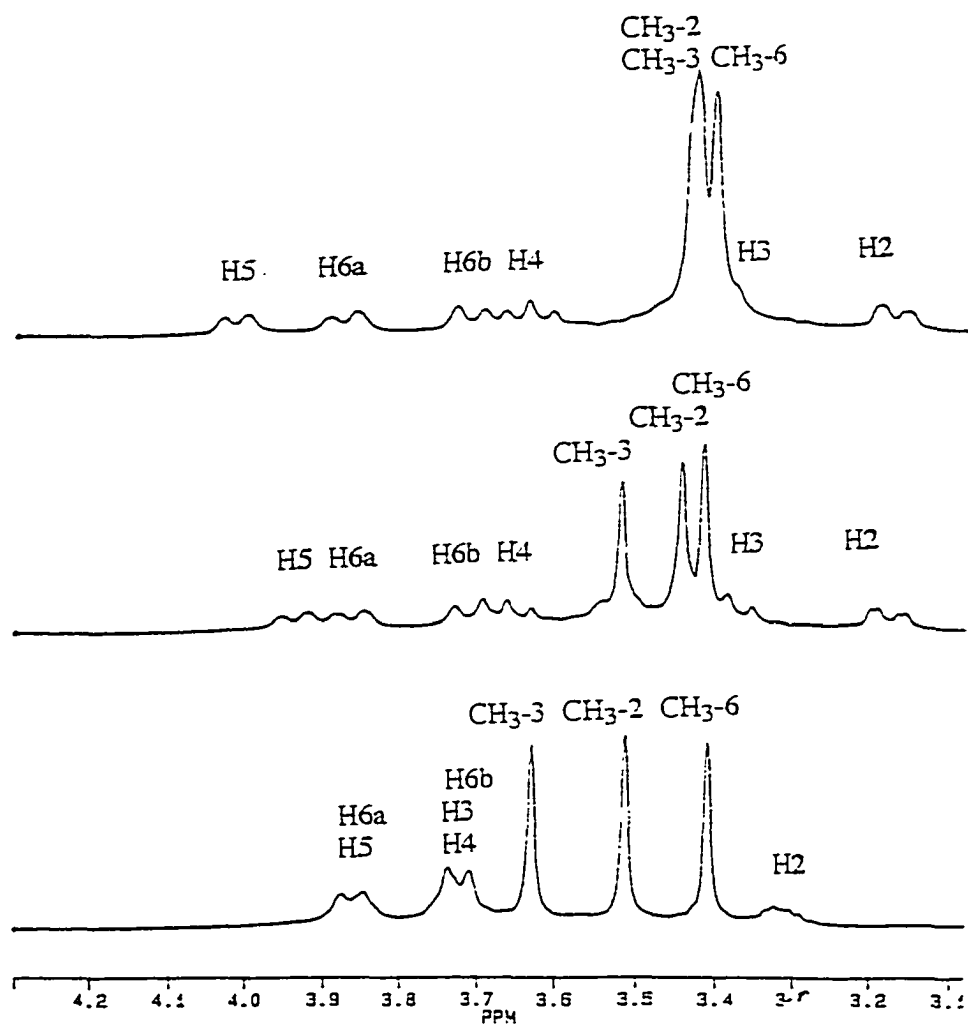


**Figure 6.** Comparison of the spectrum of  $\alpha$ -MCD (bottom) with the spectra of mixture of 4-NP (middle) and 2,6-DM-4-NP (top) at 1:3 molar ratios each.

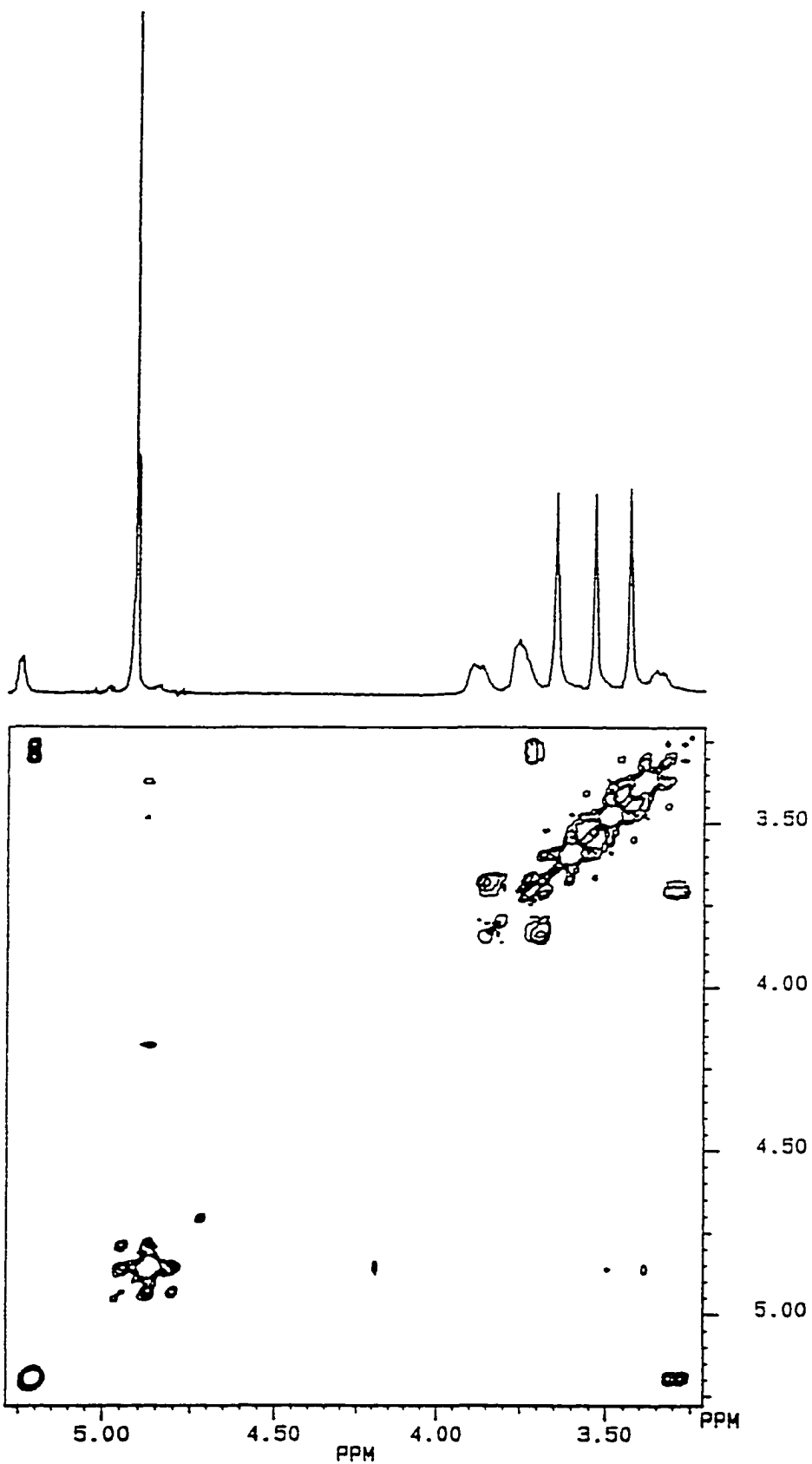


**Figure 7.** 300 MHz  $^1\text{H}$  COSY spectrum of  $\alpha$ -MCD.

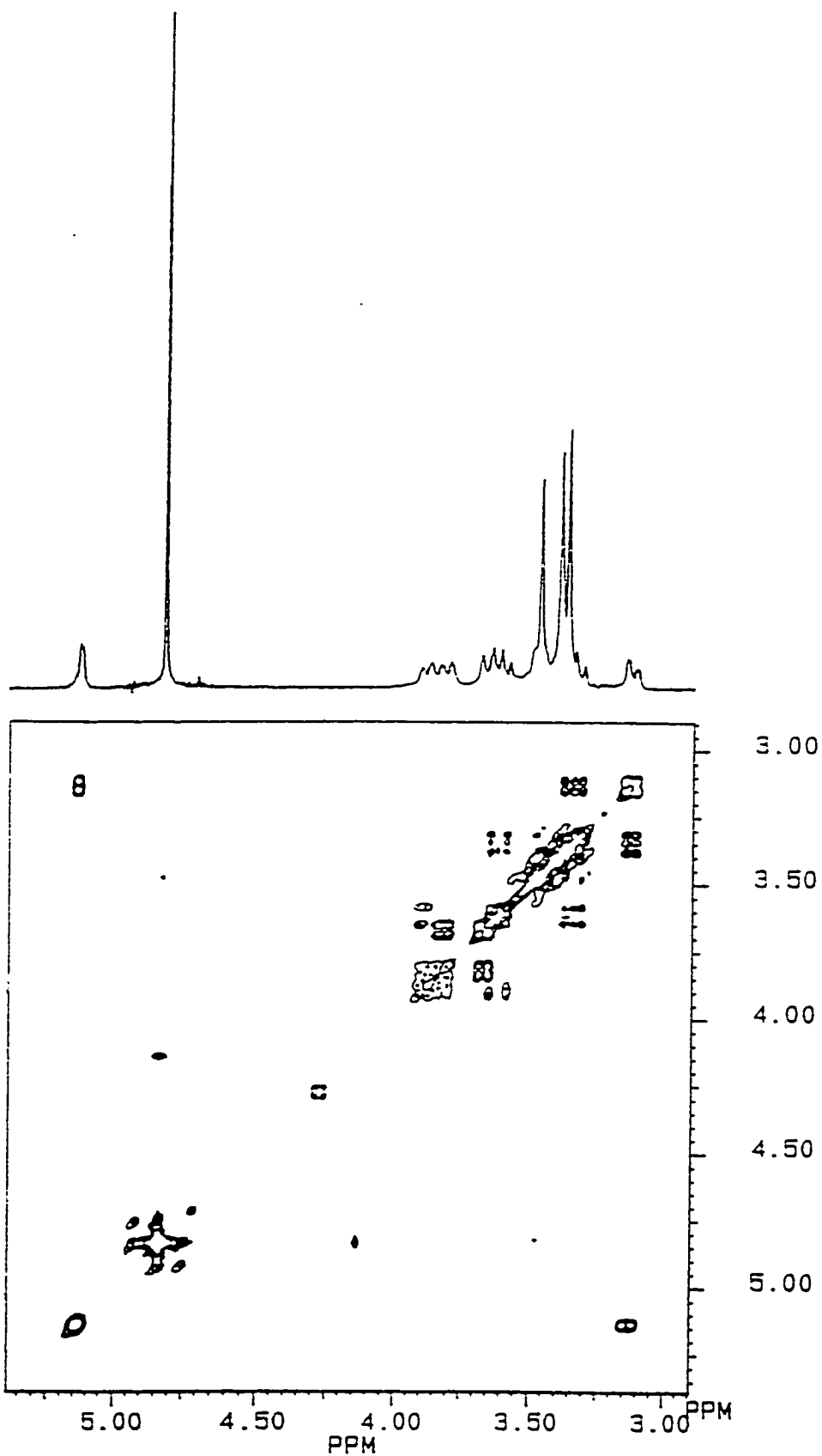


**Figure 8.** 300 MHz  $^1\text{H}$  COSY spectrum of  $\alpha$ -MCD complex with 4-NP.

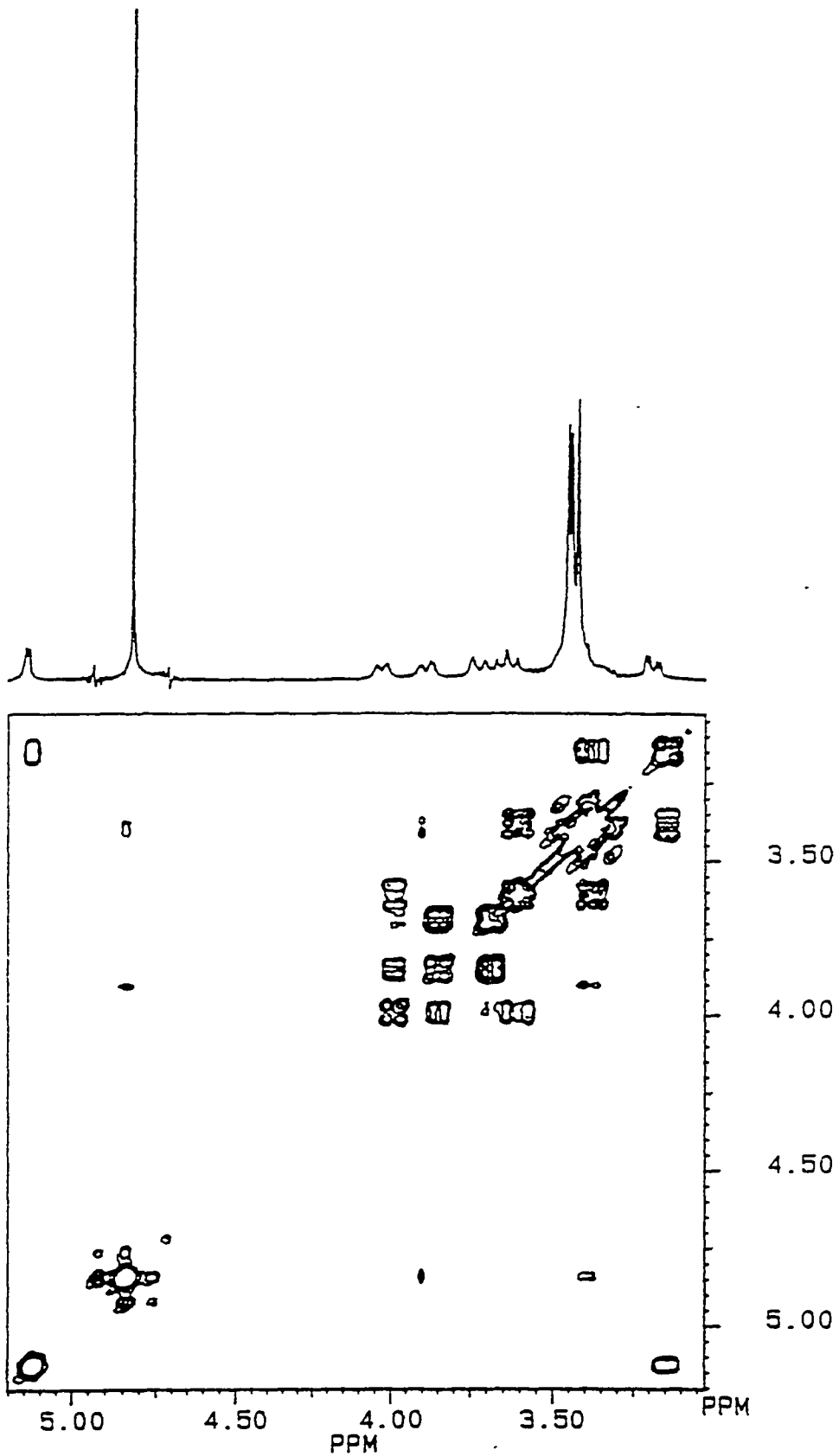


Figure 9. 300 MHz  $^1\text{H}$  COSY spectrum of  $\alpha$ -MCD complex with 2,6-DM-4-NP.

shift changes may be attributed to the distortions of  $\alpha$ -MCD discussed before for the solid state.<sup>52</sup> Although the distortion in the solid state is evident from the X-ray crystallographic studies, it is not observed in solution because the fast exchange among local distortions gives an NMR spectrum in which the signals observed are due to a single glucose unit. When a guest molecule is included in the cavity, the distortions in the conformation of  $\alpha$ -MCD are probably amplified, so that all CD protons become exposed to the new environment, but the inner ones (H-3 and H-5) are most affected. Based on  $^1\text{H}$  NMR spectra, the same trend in  $^1\text{H}$  chemical shift displacements indicates that the orientation of the 2,6-DM-4-NP molecule is quite similar to that of the 4-NP in the  $\alpha$ -MCD complex.

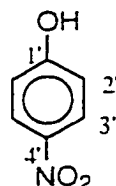
It has been found that the  $^1\text{H}$  NMR is very useful in obtaining direct evidence of the complexation. In effect, when inclusion occurs, the inner protons of the CD cavity, H-3 and H-5, in most of the cases experience a upfield shift, whereas the outer protons are much less affected. The changes in chemical shifts of the H-3 and H-5 resonances of CDs induced by a nitrophenol guest can provide information on the structure of CD complexes in solution based on the ring-current effect. However, the shift variations of the protons involved may also derive from other interactions such as magnetic anisotropy effects arising from the substituents of the guests.<sup>56</sup> The macrocyclic ring of the CD molecule may undergo conformational changes upon inclusion which could give rise to shift

variations of protons. These shift variations are not directly involved in the complexation. In an effort to confirm that the geometry of the inclusion complexes of 4-nitrophenols with  $\alpha$ -CD and  $\alpha$ -MCD, the  $^{15}\text{N}$ - $\{^1\text{H}\}$  NOE,  $^{15}\text{N}$   $T_1$  and NOESY experiments, which will be discussed in the following sections, were employed.

## 2.2 Cyclodextrin-induced Chemical Shift Changes in the $^{13}\text{C}$ and $^{15}\text{N}$ NMR of 4-Nitrophenol (4-NP)

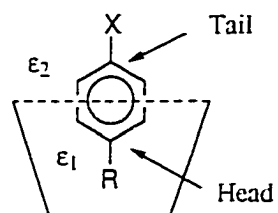
It is well known that NMR chemical shifts of organic molecules in solution are affected not only by the chemical and stereochemical structure, but also by the environment surrounding them. In NMR, the environmental effects can be theoretically treated as solvent effects.<sup>57,58</sup> The intermolecular solute-solvent interactions may be attributed to nonspecific interaction forces such as Van der Waals effects, neighbor anisotropic susceptibility, and electric field effects, as well as specific interactions including hydrogen bonding, ionic interactions, and molecular associations.<sup>57</sup> The significant variations in chemical shift observed for the solute in different solvents reflect the solvent interactions and provide a sensitive probe for studying the nature of the molecular surroundings.<sup>57,59</sup> In this study CD-induced chemical shift changes for the guest molecules (solute) may be considered to result by the transference of the guest molecule from the free state,

Table III Cyclodextrin Complexation-Induced  $^{13}\text{C}$  and  $^{15}\text{N}$  Chemical Shift Changes in 4-NP



guest	host	$^{13}\text{C}$ chemical shift changes, $\Delta\delta$ (ppm) <sup>a</sup>		$^{15}\text{N}$ chemical shift changes, $\Delta\delta$ (ppm) <sup>b</sup>
		C-1'	C-4'	$^{-15}\text{NO}_2$
4-NP	$\alpha$ -CD	+7.0	-3.7	-0.88
4-NP	$\beta$ -CD	+5.7	-3.2	-0.35

<sup>a</sup>  $^{13}\text{C}$  chemical shifts are reported with respect to  $\text{CDCl}_3$  with 1% TMS as an external reference (77.00 ppm for  $\text{CDCl}_3$  refers to 0.00 ppm for TMS). The minus and plus signs indicate high- and low-field shifts, respectively. <sup>b</sup>  $^{15}\text{N}$  chemical shifts are reported with respect to saturated  $^{15}\text{NH}_4^{15}\text{NO}_3$  aqueous solution as an external reference (21.60 ppm for  $^{15}\text{NH}_4^+$  and 375.80 ppm for  $^{15}\text{NO}_3^-$  refers to 0.00 ppm for  $^{15}\text{NH}_3$ ).



**Figure 10.** The binding of an aromatic guest molecule with  $\alpha$ -CD is modeled by a biphasic field of two different dielectric constants.

surrounded by polar water molecules, to the relatively nonpolar CD cavity (the solvent).

$^{13}\text{C}$  NMR studies of  $\alpha$ -CD complexes with some substituted benzenes by Inoue, Okuda, Miyata and Chujo<sup>56</sup> have shown that a variety of these benzenes exhibit quite similar  $^{13}\text{C}$  displacements in which the included C-4' (head carbons) are largely shielded compared to the deshielding experienced by the corresponding *para* carbons (tail carbons). Based on the  $^{13}\text{C}$  NMR data illustrated in Figure 10, the orientation of the guest molecules in the cyclodextrin cavity was determined. Neglecting the steric interaction on the guest molecule inside the cavity, they interpreted the NMR shieldings as solvent effects.<sup>56</sup>

The electrical environmental effects exerted by the non-polar CD cavity can be explained if the CD cavity is treated as a "double-layer" model,<sup>49,60</sup> in which the cavity of the cyclodextrin is assigned a dielectric constant  $\epsilon_1$  and the exterior layer is assigned a dielectric constant  $\epsilon_2$ , where  $\epsilon_1$  is much smaller than  $\epsilon_2$  ( $\epsilon_1 \ll \epsilon_2$ ). This model shown in Figure 10 could explain the typical  $^{13}\text{C}$  shift displacements observed by transference of the guest molecule from the free state in the polar aqueous environment to the relatively non-polar interior of the CD molecule.

In the present study we found that the nitrogen connected to the head carbon also undergoes a significant high-field shift upon inclusion into the  $\alpha$ - and  $\beta$ -CD cavities as shown in Table III, in which both the included

head carbon (C-4') and the nitrogen in nitro group have a significant high-field shift compared to the low-field shift of the corresponding tail carbon (C-1'). As discussed above, there are several kinds of nonspecific interactions which may influence the chemical shifts of a given nucleus.<sup>58,61</sup> Among them, the electric field effects are expected to be major contributors to the  $\alpha$ -CD and  $\beta$ -CD complexation-induced  $^{13}\text{C}$  displacements of head (C-4') and tail (C-1') carbons and  $^{15}\text{N}$  chemical shift changes of nitrogen in 4-NP.<sup>45</sup> A comparison of the  $^{15}\text{N}$  shifts based on the solvent effect model with the  $^{13}\text{C}$  high-field shifts of head (C-4') carbon supports the conclusion that the nitro group of the guest molecule is embedded in a low dielectric medium causing a different magnetic environment. In other words, the nitro group penetrates the cyclodextrin cavity as demonstrated by  $^1\text{H}$  NOE experiments.<sup>31,49</sup>

### 2.3 Determination of the Host-Guest Orientation in the Cyclodextrin (CD) Inclusion Complexes with 4-nitrophenols Using Homonuclear 2D NOE Spectroscopy (NOESY)

Measurement of the host-guest intermolecular  $^1\text{H}$  homonuclear Overhauser effect allows the qualitative determination of the orientation of the guest molecule inside the cyclodextrin cavity. The orientation of the 4-NP molecule inside the  $\alpha$ -CD cavity has been determined on the basis of

a two-dimensional NOE (NOESY) spectrum by Inoue, Yamamoto, Onda and Kitagawa,<sup>48</sup> in which the cross-peaks connect the H-3 resonance of  $\alpha$ -CD to both the protons *meta* and *ortho* to 4-nitrophenolic hydroxyl group, while a cross-peak connects the H-5 only to the *meta* proton resonance. In our work, NOESY studies also extend to inclusion complexes of  $\alpha$ -CD with 2,6-DM-4-NP and  $\alpha$ -MCD with 4-NP, and 2,6-DM-4-NP.

The NOESY and  $^1\text{H}$  NMR spectra of the  $\alpha$ -CD complex with 2,6-DM-4-NP in alkaline buffer solution (pD 11) are illustrated in Figure 11. In the NOESY spectrum, the cross-peaks connect the H-3 resonance of  $\alpha$ -CD to both the H-3' proton (*meta* to nitrophenolic hydroxyl group) and  $\text{CH}_3$ -proton resonances of 2,6-DM-4-NP, while a cross-peak connects the H-5 resonance only to the H-3' resonance although the intensity of this signal is lower than that of the former ones. Specifically, the intensity of a NOE cross-peak depends not only on the distance between the nuclei involved, but also on the value of the mixing time,  $\tau_m$ , during which the NOE develops and the zero-quantum coherence giving rise to COSY-type cross-peak is reduced.<sup>46</sup> Since the NOESY experiments in this study were performed with different values of  $\tau_m$  so as to optimize the spectrum, it is reasonable to assume that the weak cross-peak connecting the H-5 resonance of  $\alpha$ -CD to the H-3' resonance of the guest is due to the longer distance between these correlated hydrogens than those between H-3 of  $\alpha$ -CD and guest protons. These results indicate that 2,6-DM-4-NP is

incorporated into the cavity of the  $\alpha$ -CD with the nitro head first, and further support the explanations<sup>51</sup> given for the complexation-induced  $^1\text{H}$  chemical shift changes. that is, the H-3 resonance is shielded and the H-5 is deshielded. suggesting the guest penetrates less deeply into the cavity.

The NOESY and  $^1\text{H}$  NMR spectra of  $\alpha$ -MCD-4-NP and  $\alpha$ -MCD-2,6-DM-4-NP complexes in an alkaline buffer solution (pD11) are shown in Figures 12 and 13. respectively. Figure 12 shows cross-peaks connecting the H-3 resonance of  $\alpha$ -MCD to both the *meta* and *ortho* proton resonances of 4-NP. However, in contrast to  $\alpha$ -CD, there is no cross-peak connecting the H-5 resonance in  $\alpha$ -MCD to the proton resonances in 4-NP. It was confirmed by performing the experiments with different values of  $\tau_m$ , which result in optimizing the NOESY spectrum. The absence of such a cross-peak suggests a longer distance between the H-5 hydrogens and the hydrogens of 4-NP. This observation is reasonable if 4-NP is inserted into the cavity of  $\alpha$ -MCD from the nitro group and the depth of penetration of 4-NP into the  $\alpha$ -MCD cavity is less than the depth of penetration of 4-NP into the  $\alpha$ -CD cavity. As explained before for the solid state, in  $\alpha$ -MCD the size of the secondary methoxy side of the cavity is widened, while the primary methoxy side is narrowed so that the nitrophenyl group can not be deeply inserted, possibly due to steric hindrance of the nitro group of 4-NP with the H-5 hydrogens of  $\alpha$ -MCD. This cone shape of  $\alpha$ -MCD in solution

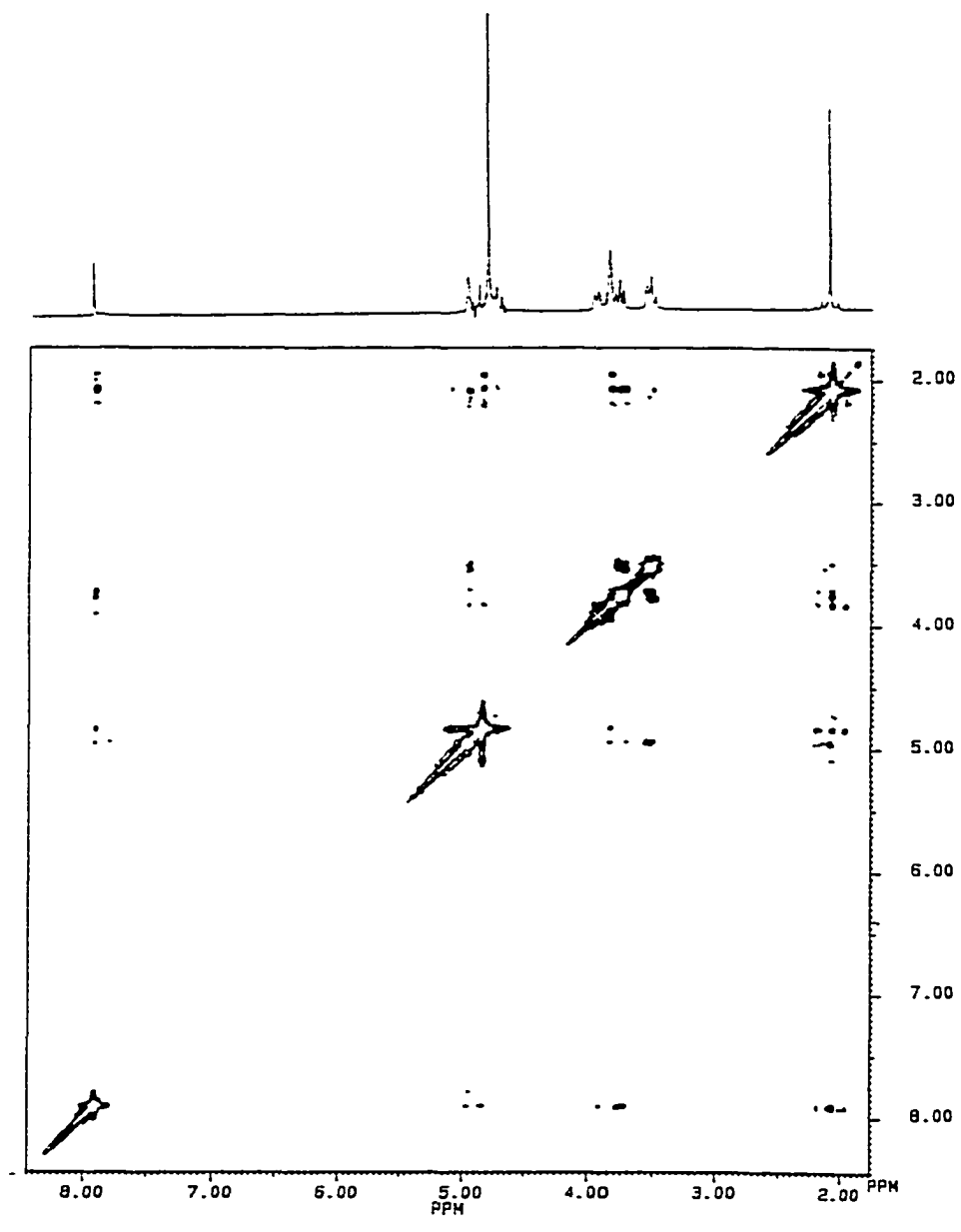


**Figure 11.** 300 MHz NOESY spectrum of  $\alpha$ -CD inclusion complex with 2,6-DM-4-NP.

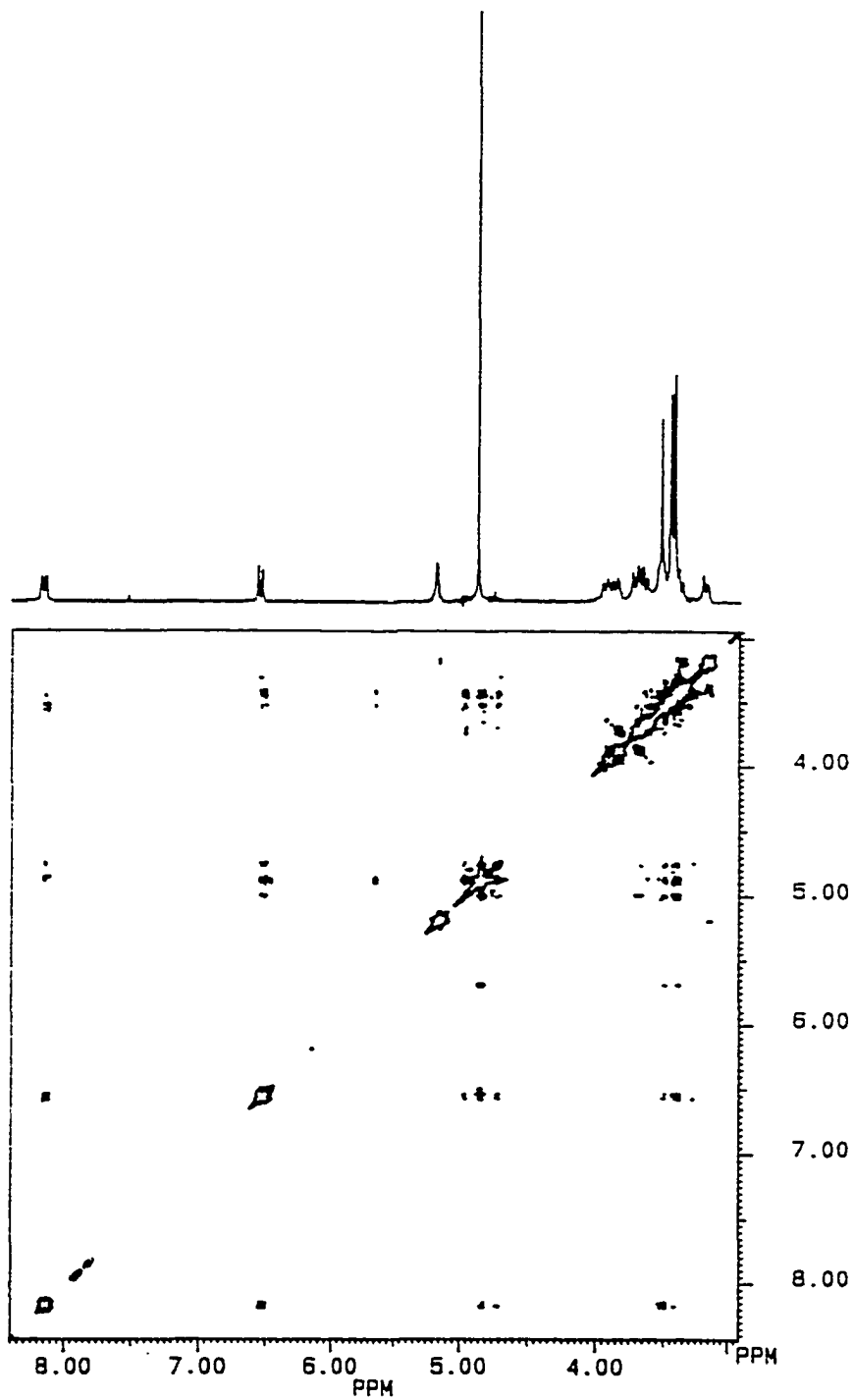
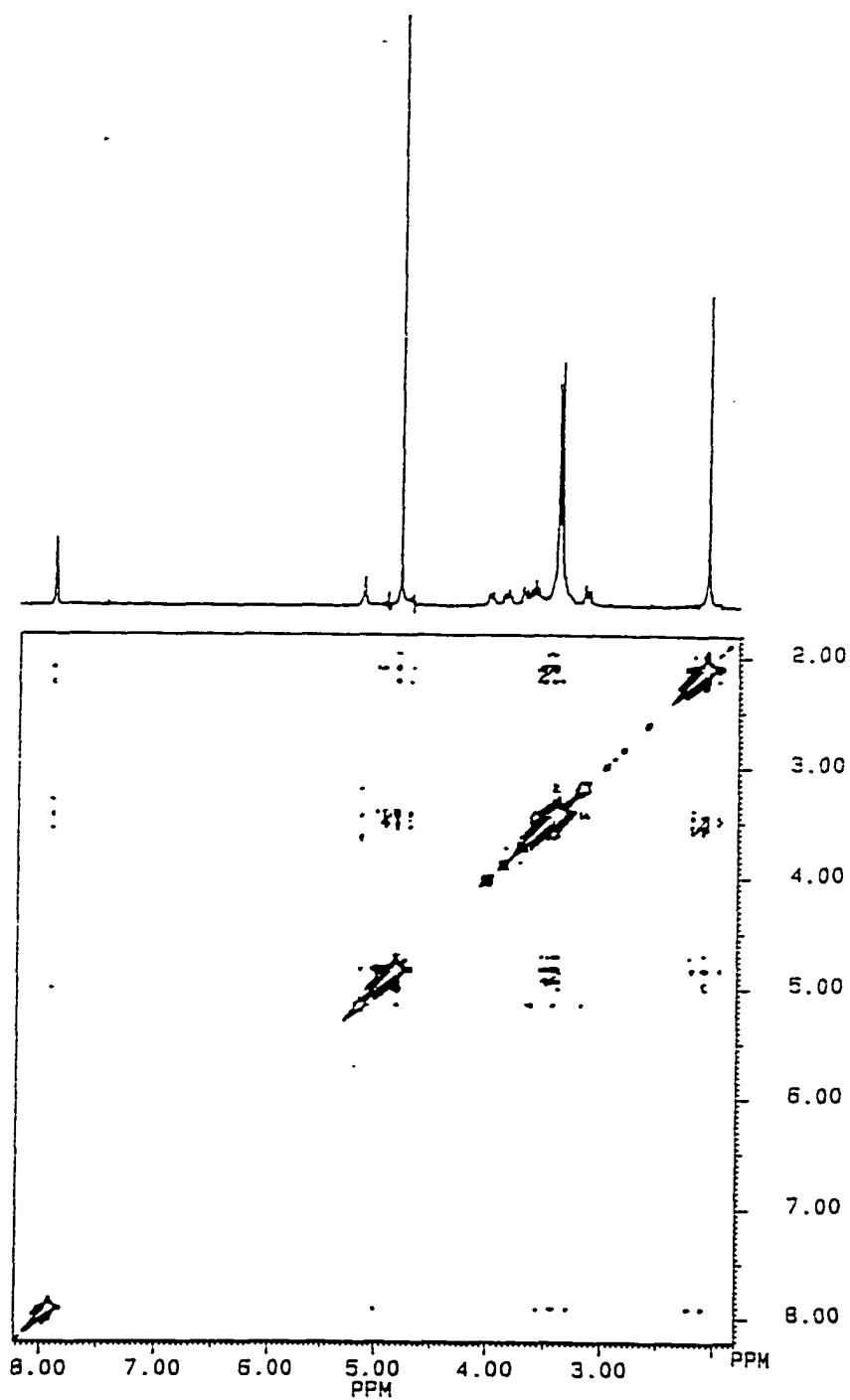


Figure 12. 300 MHz NOESY spectrum of  $\alpha$ -MCD complex with 4-NP.



**Figure 13.** 300 MHz NOESY spectrum of  $\alpha$ -MCD complex with 2,6-DM-4-NP.

is consistent with that described in the solid state as determined by X-ray diffraction.<sup>52</sup>

The NOESY spectrum shown in Figure 13 for the complex of  $\alpha$ -MCD with 2,6-DM-4-NP resembles that of the 4-NP complex. Specifically, the H-3 resonance of  $\alpha$ -MCD correlates with both the CH<sub>3</sub>- and H-3'-proton resonances of 2,6-DM-4-NP, while the H-5 resonance does not correlate with any proton resonances for the guest molecule. With regard to the geometrical features of the host-guest complexes, the <sup>1</sup>H-<sup>1</sup>H NOESY experiments demonstrate that the host-guest orientation for the 2,6-DM-4-NP complex is similar to that proposed for the 4-NP complex.

Although the apolar cavity of  $\alpha$ -MCD has a great affinity towards the phenyl ring of 4-nitrophenols, the absence of a connection between the H-5 resonance in  $\alpha$ -MCD and the proton resonances in 4-nitrophenols can be attributed to the weak dipolar interactions between them due to the change of the cone shape of  $\alpha$ -MCD as discussed above. It is expected that the heteronuclear intermolecular dipole-dipole interaction between the <sup>15</sup>N atoms in 4-nitrophenols and the inner protons in  $\alpha$ -MCD will be large enough to be measured due to the large magnitude of the <sup>15</sup>N resonance enhancement (maximum 400%). In our work, the host-guest geometry for the  $\alpha$ -MCD complexes with 4-nitrophenols was determined using <sup>15</sup>N-<sup>1</sup>H heteronuclear NOE experiment.

## 2.4 $^{15}\text{N}\{-^1\text{H}\}$ Heteronuclear NOE as a Probe of Host-Guest Geometry in Cyclodextrin (CD) Inclusion Complexes with 4-Nitrophenols (4-NPs)

The  $^{15}\text{N}\{-^1\text{H}\}$  heteronuclear Overhauser experiments with  $^{15}\text{N}$ -enriched samples of 4-NP and 2,6-DM-4-NP in the presence of  $\alpha$ -CD were carried out at 20 MHz for  $^{15}\text{N}$ . The enhancements of the  $^{15}\text{N}$  resonances in 4-NP and 2,6-DM-4-NP were observed upon irradiation at both the H-3 and the H-5 resonances in the  $\alpha$ -CD. Unambiguous intermolecular NOE data established that heteronuclear dipole cross-relaxation also takes place inside the cyclodextrin cavity. The heteronuclear NOE difference spectra are provided in Figure 14 and Figure 15 for time-averaged  $\alpha$ -CD-4-NP and  $\alpha$ -CD-2,6-DM-4-NP inclusion complexes, respectively. Table IV summarizes the  $^{15}\text{N}\{-^1\text{H}\}$  NOE experiments for 4-NP- $\alpha$ -CD and 2,6-DM-4-NP- $\alpha$ -CD inclusion complexes. At 200 MHz, the separation of H-3 and H-5 resonances (30 Hz) makes it possible to saturate individual cyclodextrin resonances in which the decoupler power is carefully controlled so it does not partially saturate neighboring resonances.

The theory of intermolecular NOE in rapidly exchanging systems was presented by Neuhaus and Williamson.<sup>62</sup> In general, quantitative interpretation of intermolecular NOE in exchanging systems may be quite complex. In the present case, however, the situation is simplified since the nitrophenol guest is in rapid equilibrium between the free state and the

**Table IV. Heteronuclear  $^{15}\text{N}$ - $\{^1\text{H}\}$  NOE Data from  $\alpha$ -CD Complexes<sup>a</sup> with 4-Nitrophenols- $^{15}\text{N}$**

guest	host	$\%^{15}\text{N}$ enhancement <sup>b</sup> on irradiation of	
		H-3	H-5
4-NP	$\alpha$ -CD	16	59
2,6-DM-4-NP	$\alpha$ -CD	25	39

<sup>a</sup>  $^{15}\text{N}$  heteronuclear NOE was observed in buffer solution containing 0.068 M  $\alpha$ -CD and 0.045 M 4-NP or 2,6-DM-4-NP. <sup>b</sup> Reported values represent the average of values calculated from the signal intensities of three experiments; estimated accuracy  $\pm 6\%$ .





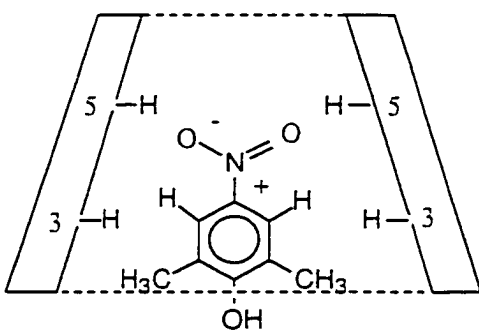
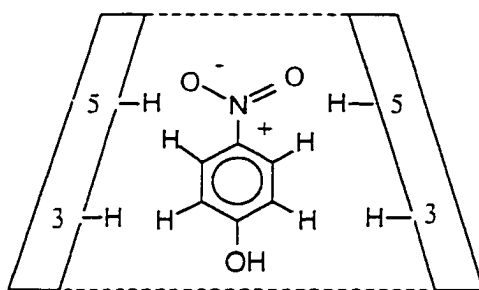


**Figure 16.** Schematic representation of the host-guest orientation in the  $\alpha$ -CD inclusion complexes with (top) 4-NP and (bottom) 2,6-DM-4-NP.

complexed state. The NOE enhancements can be obtained by averaging the cross-relaxation rates for the free and bound guests, allowing only a single  $^{15}\text{N}$  signal of the nitro group to be observed. The 4-NP and 2,6-DM-4-NP in the samples were over 99% bound to the  $\alpha$ -CD.<sup>3</sup> Thus, the mole fraction of the observed species in the bound state was large enough that NOE intensity changes were seen in the averaged (free plus bound) spectrum. The magnitude of the observed NOE is dependent on the extent to which the  $^{15}\text{N}$  nucleus, whose resonance is being observed, is relaxed by the  $\alpha$ -CD  $^1\text{H}$  nucleus whose resonance is being irradiated. The requirements for the observation of NOE are that the two nuclei be close to one another, and that they remain in close proximity long enough for intermolecular relaxation to occur.

Since the  $^{15}\text{N}$  resonance of 4-NP showed a much larger enhancement (59%) when the H-5 resonance in the  $\alpha$ -CD was irradiated than when the H-3 resonance was irradiated (16%) as shown in Table IV, we conclude that the H-5 protons contribute more to the relaxation of the  $^{15}\text{N}$  nucleus than the H-3 protons. It is known that internuclear dipole-dipole relaxation rates have  $1/r^6$  dependence on the distance  $r$  between the relaxed nucleus and the nucleus causing relaxation.<sup>36</sup> This is best explained if one assumes that the 4-NP penetrates the cavity to the extent that its nitrogen is in intimate contact with the H-5 proton, but at a substantially greater distance

from H-3. These results support the previous conclusion that the geometry of the  $\alpha$ -CD-4-NP complex in solution is as shown in Figure 16.

Irradiation at the H-5 and H-3 resonances in  $\alpha$ -CD showed a 39% and a 25% enhancement, respectively, for the  $^{15}\text{N}$  resonance of 2,6-DM-4-NP. These results place the nitrogen of the guest 2,6-DM-4-NP between the H-5 and H-3 protons. However, the result from a comparison of the NOE (59%) obtained from the  $^{15}\text{N}$  resonance in 4-NP after irradiation of H-5 in the  $\alpha$ -CD with the smaller NOE (39%) observed for the  $^{15}\text{N}$  resonance in 2,6-DM-4-NP can be interpreted as a decrease in the depth of penetration for 2,6-DM-4-NP. The position of the 2,6-DM-4-NP in  $\alpha$ -CD cavity is illustrated qualitatively in Figure 16. Clearly, introduction of two methyl groups in positions 2 and 6 in the 4-NP provides an effective steric barrier to limit substrate penetration. The position of the 2,6-DM-4-NP in the  $\alpha$ -CD cavity determined by the heteronuclear NOE agrees well with the results of corresponding  $^1\text{H}$  chemical shift changes. Namely, the shielding of the  $\alpha$ -CD H-3 protons was the same as that observed for the  $\alpha$ -CD-4-NP complex. However, the H-5 proton resonance was strongly deshielded by the two nitro oxygens in the substrate.

The NOE difference spectra are shown in Figure 17 for  $\alpha$ -MCD-4-NP and in Figure 18 for the  $\alpha$ -MCD-2,6-DM-4-NP complexes. Table V summarizes the  $^{15}\text{N}$ - $^1\text{H}$  NOE experiments of 4-NP- $\alpha$ -MCD and 2,6-DM-4-NP- $\alpha$ -MCD inclusion complexes. In the  $^1\text{H}$  NMR spectra, complexations of

$\alpha$ -MCD with 4-NP and 2,6-DM-4-NP induce 0.33 ppm and 0.31 ppm up-field shifts for the H-3 protons, respectively, and 0.11 and 0.14 ppm down-field shifts for the H-5 protons, respectively. This separation of the H-3 and H-5 resonances permits selective irradiation, in which the relatively high irradiation power can be used to fully saturate the protons in order to maximize NOE. The  $^{15}\text{N}$ - $^1\text{H}$  heteronuclear NOE experiments were performed on the  $\alpha$ -MCD-4-NP and the  $\alpha$ -MCD-2,6-DM-4-NP complex to a 99% substrate bound.<sup>31,49</sup>

A 71% enhancement in the  $^{15}\text{N}$  resonance of 4-NP was generated with an irradiation power of 0.10 watt when the H-5 resonance in the  $\alpha$ -MCD-4-NP complex was irradiated. In contrast, a 7% enhancement occurred when the H-3 resonance was irradiated. These results, shown in Table V, indicate that the nitro group of the 4-NP penetrates the cavity to the extent that the nitrogen atom is closer to H-5 than H-3 in the  $\alpha$ -MCD cavity. The position of 4-NP in cavity is presented in Figure 19. Thus, these results further confirm the conclusion from the NOESY study, and are consistent with those of the  $^1\text{H}$  NMR study for the  $\alpha$ -MCD-4-NP complex.

A 54% enhancement in the  $^{15}\text{N}$  resonance of 2,6-DM-4-NP was generated with a irradiation power of 0.11 watt when the H-5 resonance in the  $\alpha$ -MCD complex was irradiated and a 16% enhancement was generated when the H-3 resonance was irradiated. These results support the

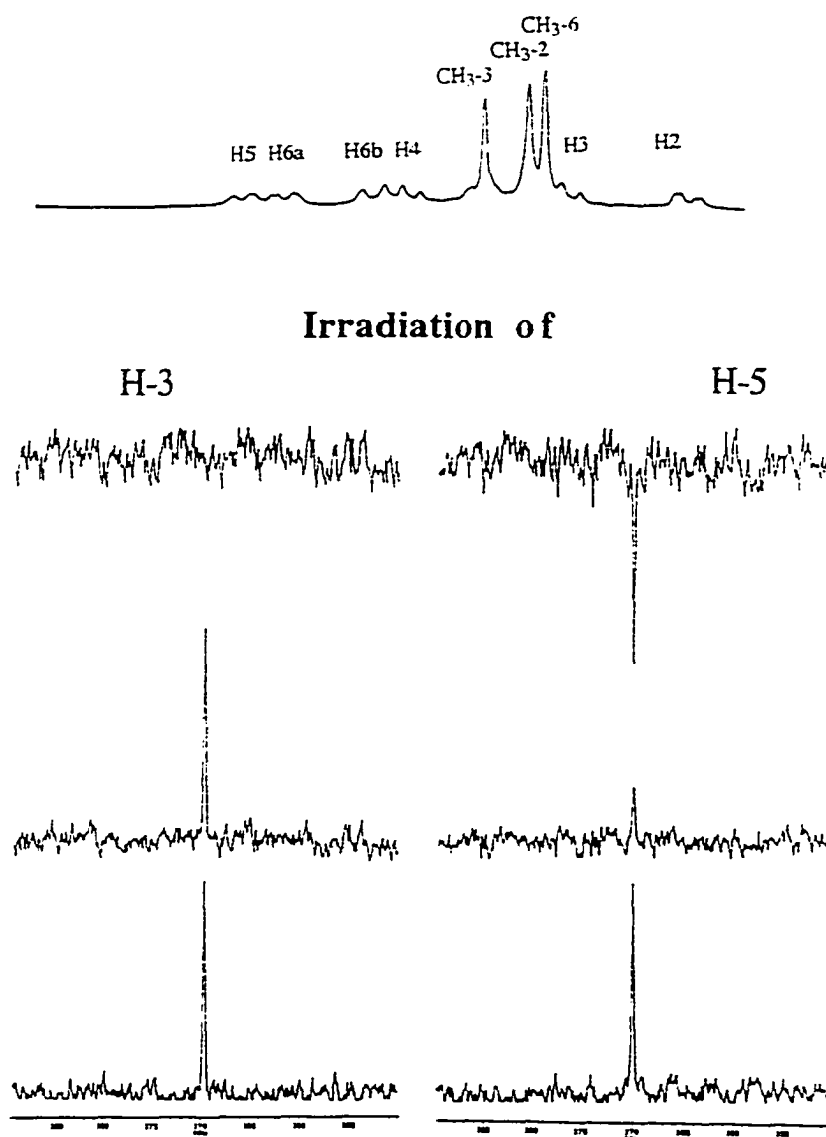


**Figure 17.** 20 MHz heteronuclear  $^{15}\text{N}\{-^1\text{H}\}$  NOE difference spectra for the  $\alpha$ -MCD complex with 4-NP- $^{15}\text{N}$ . The intermolecular nuclear Overhauser enhancement of the  $^{15}\text{N}$  atom in 4-NP upon irradiation of H-3 and H-5 is shown in difference spectra. In each set of spectra, the bottom one is the reference where the irradiating rf was set far from the resonance of the sample. The  $^{15}\text{N}$  difference spectrum (top of each set) was obtained by subtraction of the reference from the middle spectrum where H-3 and H-5 of  $\alpha$ -MCD were subjected to irradiation, respectively.

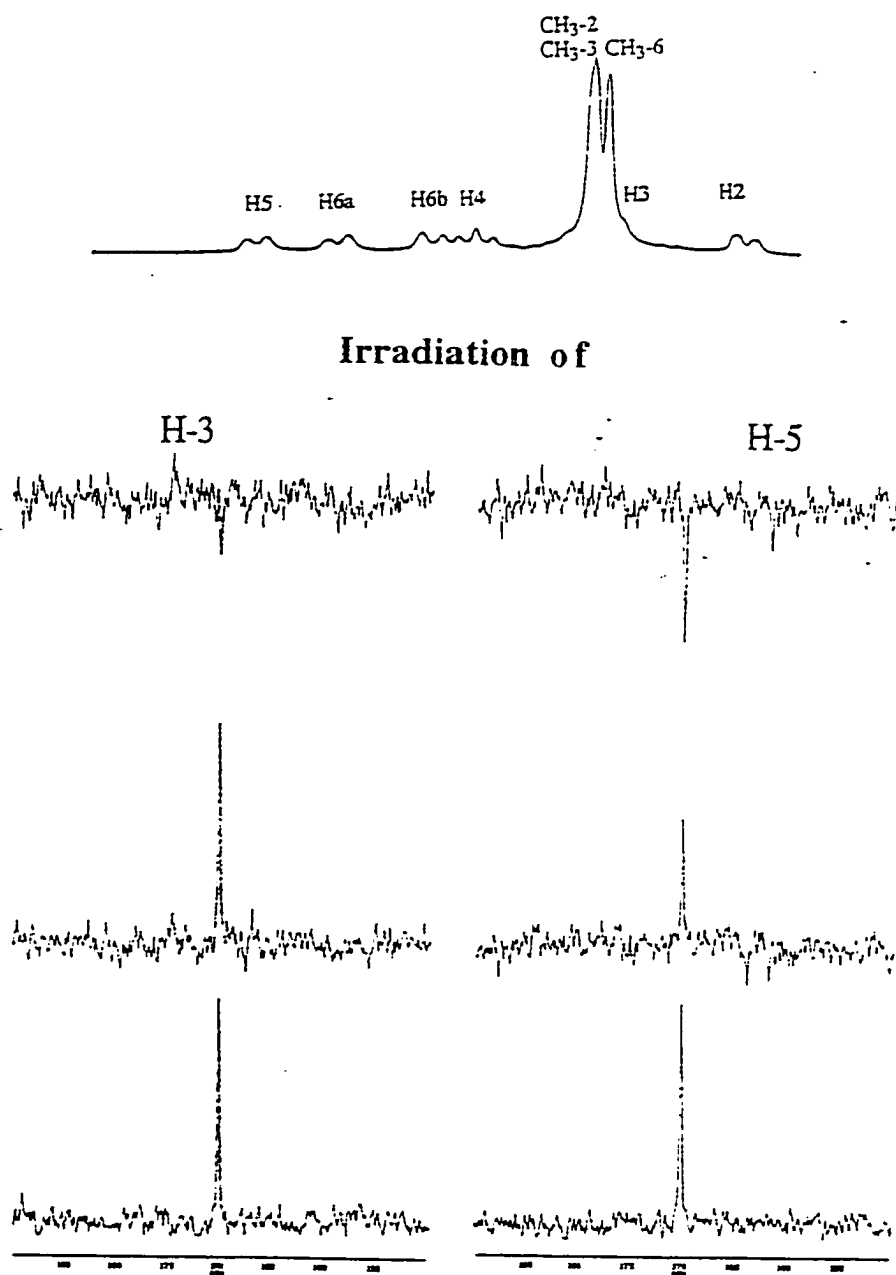


**Figure 18.** 20 MHz heteronuclear  $^{15}\text{N}\{-^1\text{H}\}$  NOE difference spectra for the  $\alpha$ -MCD complex with 2,6-DM-4-NP- $^{15}\text{N}$ . The intermolecular nuclear Overhauser enhancement of the  $^{15}\text{N}$  atom in 2,6-DM-4-NP upon irradiation at H-3 and H-5 is shown in difference spectra. In each set of spectra, the bottom one is a reference where the irradiating rf was set far from the resonance of the sample. The  $^{15}\text{N}$  difference spectrum (top of each set) was obtained by subtraction of the reference from the middle spectrum where H-3 and H-5 of  $\alpha$ -MCD were subjected to irradiation, respectively.

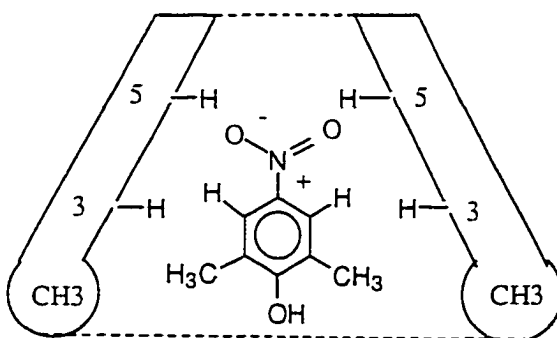
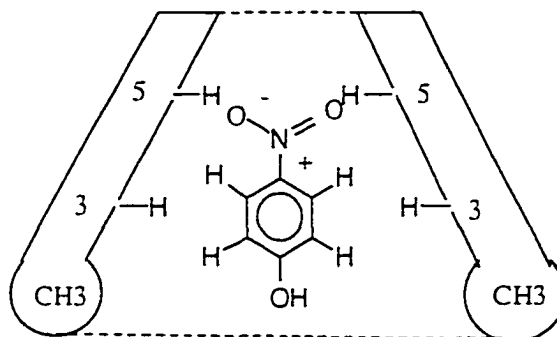
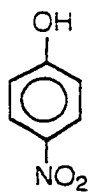


**Figure 19.** Schematic representation of the host-guest orientation in the  $\alpha$ -MCD inclusion complexes with (top) 4-NP and (bottom) 2,6-DM-4-NP.

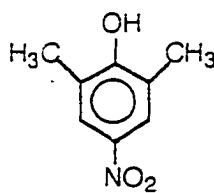
**Table V. Heteronuclear  $^{15}\text{N}$ - $\{^1\text{H}\}$  NOE Data from  $\alpha$ -MCD  
Complexes with 4-Nitrophenols- $^{15}\text{N}$**

guest	host	% $^{15}\text{N}$ enhancement <sup>a</sup> on irradiation of	
		H-3	H-5
<b>1a</b>	$\alpha$ -MCD	7	71
<b>1b</b>	$\alpha$ -MCD	16	54

<sup>a</sup> Reported values represent the average of values calculated from the signal intensities of three experiments; estimated NOE accuracy  $\pm 6\%$ .



**1a**



**1b**

**Table VI. The NOE Enhancement with Different Irradiation Power**

guest	host	Irradiation power (Watt)	% <sup>15</sup> N enhancement on	
			Irradiation of	
			H-3	H-5
<b>1a</b>	$\alpha$ -CD	0.08	16	59
<b>1a</b>	$\alpha$ -MCD	0.10	7	71
		0.08	0	0
<b>1b</b>	$\alpha$ -CD	0.09	25	39
<b>1b</b>	$\alpha$ -MCD	0.11	16	54
		0.09	0	0

conclusion from the NOESY and  $^1\text{H}$  NMR studies of the  $\alpha$ -MCD-2,6-DM-4-NP complex. e.g. the depth of penetration of 2,6-DM-4-NP into the cavity is less than that of 4-NP. The position of the 2,6-DM-4-NP in the cavity is presented in Figure 19.

In Table VI the respective effects of irradiation power on the  $\alpha$ -CD and  $\alpha$ -MCD complexes show that the  $\alpha$ -MCD complexes require more irradiation power to saturate the H-3 and H-5 protons than the  $\alpha$ -CD complexes. Since the extent of the NOE observed is proportional to the irradiation power used, it can be suggested that the intermolecular hydrogen-nitrogen distance is longer in the  $\alpha$ -MCD cavity than in the  $\alpha$ -CD cavity due to the widening of the hydrophobic region of the CD cavity after methylation as discussed before for the solid state. It leads to a conclusion that the structures of the macrocycle of  $\alpha$ -MCD upon inclusion of 4-nitrophenols in solution resemble those in the solid state.

The proposed geometries suggested for the  $^{15}\text{N}$ -{H} NOE for the  $\alpha$ -MCD complexes indicate that  $\alpha$ -MCD includes 4-nitrophenols in the same manner as  $\alpha$ -CD. Therefore, the 4-NP and the 2,6-DM-4-NP are expected to bind quite rigidly to both the  $\alpha$ -MCD and  $\alpha$ -CD. This binding rigidity is supported by  $^{15}\text{N}$   $T_1$  experiment.

## 2.5. $^{15}\text{N}$ Spin-lattice Relaxation Time ( $T_1$ ) of Cyclodextrin (CD) Inclusion Complexes with 4-Nitrophenols (4-NPs)

The  $^{15}\text{N}$  spin-lattice relaxation times of the free 4-NP, 2,6-DM-4-NP, and their respective complexes with  $\alpha$ - and  $\beta$ -CDs are given in Table VII. The  $T_1$  values are dependent on the viscosity of the solution.<sup>62</sup> Therefore, the viscosity of the uncomplexed solutions has been compensated by adding seven molar portions of methyl- $\alpha$ -D-glucopyranoside. Table VIII shows the ratios of the  $T_1$  values for the free and complexed states of the 4-NP and 2,6-DM-4-NP.

According to equations (3) and (4) in Chapter 1, if complex formation results in an increased correlation time of the 4-NP or 2,6-DM-4-NP guest, the  $^{15}\text{N}$   $T_1$  would be expected to decrease as the fraction of the complexed guest increases. Based on the above arguments the results, in which the  $^{15}\text{N}$   $T_1$  values for the 4-NP and 2,6-DM-4-NP are largely decreased by complexation with cyclodextrins (see Tables VII and VIII), support the fact that nitrophenols bind quite tightly with cyclodextrins in aqueous solution.

The data in Tables VII and VIII indicate that the magnitude of the  $^{15}\text{N}$   $T_1$  changes for the nitrophenols in the  $\alpha$ -CD are different from those in  $\beta$ -CD. In the  $\alpha$ -CD complex, for example, the  $^{15}\text{N}$   $T_1$  value of 4-NP

**Table VII.  $^{15}\text{N}$  Spin-lattice Relaxation Times ( $T_1$ ) of 4-NP and 2,6-DM-4-NP<sup>a</sup> in Cyclodextrin Inclusion Complexes**

guest	host	guest /host (mol : mol)	$T_1(\text{s})^b$
1a	—	—	263.6
1a <sup>c</sup>	—	1 : 10.5	222.0
1a	$\alpha$ -CD	1 : 1.5	23.3
1a	$\beta$ -CD	1 : 1.5	43.7
1b	—	—	189.4
1b <sup>c</sup>	—	1 : 10.5	138.6
1b	$\alpha$ -CD	1 : 1.5	20.6
1b	$\beta$ -CD	1 : 1.5	25.9

<sup>a</sup>  $^{15}\text{N}$   $T_1$  was observed in pD 11 buffer solution containing 0.038 M  $\alpha$ -CD and 0.025 M 4-NP or 2,6-DM-4-NP. <sup>b</sup> Reported values represent the average of values calculated from the signal intensities of three experiments; estimated  $T_1$  accuracy  $\pm 5\%$ . <sup>c</sup> Seven molar portions of methyl- $\alpha$ -D-glucopyranoside were added.

**Table VIII. Values of  $^{15}\text{N}$   $T_1$  Ratios for the Free and Complexed 4-Nitrophenols with  $\alpha$ - and  $\beta$ -Cyclodextrins**

guest	host	$T_{1\text{free}}/T_{1\text{complex}}$
<b>1a</b>	$\alpha$ -CD	9.5
<b>1b</b>	$\beta$ -CD	5.1
<b>1b</b>	$\alpha$ -CD	6.7
<b>1b</b>	$\beta$ -CD	5.4

decreases by a factor of 9.5 while that in the  $\beta$ -CD complex decreases by a factor of 5.1. Likewise, the  $^{15}\text{N}$   $T_1$  value of the 2,6-DM-4-NP decreases by a factor of 6.7 in the  $\alpha$ -CD complex and decreases by a factor of 5.4 in the  $\beta$ -CD complex. These results suggest that the 4-NP and 2,6-DM-4-NP bind more tightly to the  $\alpha$ -CD. This behavior is expected since the  $\alpha$ -CD cavity, which is smaller than that of the  $\beta$ -CD, fits the guest molecules better than the  $\beta$ -CD cavity. On the other hand, the ratio of  $T_{1\text{free}} / T_{1\text{complex}}$  in 4-NP is greater than that in 2,6-DM-4-NP in the presence of  $\alpha$ -CD, while the ratio in 4-NP is comparable to that in the 2,6-DM-4-NP in the presence of  $\beta$ -CD, as shown in Table VI. These results may be explained by the introduction of the two methyl groups in 4-NP which decreases the depth of substrate penetration in the  $\alpha$ -CD cavity as discussed in the previous sections. The larger cavity of  $\beta$ -CD, however, allows 2,6-DM-4-NP molecule for a deep penetration.

Although a host-guest orientation cannot be directly obtained from the  $^{15}\text{N}$   $T_1$ , the results, in which the  $T_1$  values of nitrogen in 4-NP and 2,6-DM-4-NP show large changes when  $\alpha$ -CD complexation occurs, are consistent with a model in which the nitrophenyl groups are tightly trapped in the  $\alpha$ -CD cavity.

The  $^{15}\text{N}$   $T_1$  values for 4-NP and 2,6-DM-4-NP in the absence and the presence of  $\alpha$ -MCD are listed in Table IX. Since the molecular volume of

**Table IX.  $^{15}\text{N}$  Spin-lattice Relaxation Times ( $T_1$ ) of 4-NP and 2,6-DM-4-NP in  $\alpha$ -MCD Inclusion Complexes.**

guest	host	guest/host (mol : mol)	$T_1$ (s)	$T_{1\text{free}} / T_{1\text{com.}}$
<b>1a<sup>a</sup></b>	—	1 : 10.5	222.0	—
<b>1a</b>	$\alpha$ -MCD	1 : 1.5	14.5	15.3
<b>1b<sup>a</sup></b>	—	1 : 10.5	138.6	—
<b>1b</b>	$\alpha$ -MCD	1 : 1.5	11.5	12.1

<sup>a</sup> Seven molar portions of methyl- $\alpha$ -D-glucopyranoside were added.

$\alpha$ -MCD is about 7 ~ 9 times larger than those of the nitrophenols. the extent of the decrease in the  $T_1$  values for 4-nitrophenols in inclusion complexes can be used as an estimation of the rigidity of binding.

Table IX shows that the  $^{15}\text{N}$   $T_1$  values for the 4-NP and 2,6-DM-4-NP are significantly decreased by complexation with  $\alpha$ -MCD. The degree of restriction of molecular motion can be estimated by calculating the ratios of  $T_1$  values for the complexed and free states of 4-nitrophenols. The larger value of this ratio, the more restriction of molecular motion of the 4-nitrophenols by complexation with  $\alpha$ -MCD. The values of ratios, which are 15.3 for 4-NP- $\alpha$ -MCD complex and 12.1 for 2,6-DM-4-NP- $\alpha$ -MCD complex, indicate that both 4-NP and 2,6-DM-4-NP form the inclusion complexes with  $\alpha$ -MCD by insertion of a nitrophenyl ring into the  $\alpha$ -MCD cavity and the molecular motions of the 4-NP and 2,6-DM-4-NP are thus greatly restricted.

A comparison of the  $T_{1\text{free}} / T_{1\text{com.}}$  ratios of  $^{15}\text{N}$   $T_1$  values for the 4-nitrophenols on addition of the  $\alpha$ -CD, as shown in Table VIII, indicates that  $\alpha$ -MCD forms the inclusion complexes in a similar manner. In other words, permethylation of hydroxyl groups in the  $\alpha$ -CD essentially does not modify the mode of the nitrophenol inclusion.

Finally, it is interesting to speculate about the correlations between the binding rigidity derived from  $^{15}\text{N}$   $T_1$  and the thermodynamic binding constants ( $K_d$ )<sup>31,49,63</sup> for cyclodextrin-nitrophenol binding. Inspection of

Tables VIII and IX shows that there is a decrease in  $T_{\text{ifree}} / T_{\text{icom.}}$  ratio for the 4-NP complexes:  $\alpha\text{-MCD-4-NP} > \alpha\text{-CD-4-NP}$ . Obviously, the binding constants show the same trends. These results imply that 4-nitrophenol is more tightly bound in the  $\alpha\text{-MCD}$  cavity than in the  $\alpha\text{-CD}$  cavity. In other words, 4-nitrophenol forms more stable inclusion complexes with  $\alpha\text{-MCD}$  than with  $\alpha\text{-CD}$ . In the general case of the guest-host complex formation, the binding force is supposed to be provided, at least partially, by hydrophobic interaction. As discussed before, the permethylation may increase the binding tendency of the apolar nitrophenyl ring to the cyclodextrin cavity if the hydrophobic interaction is the major mechanism for the formation of the inclusion complexes. The results derived from the  $K_d$ <sup>31,49,63</sup> and the  $^{15}\text{N}$   $T_1$  values for the permethylated  $\alpha\text{-CD}$  complexes support this assumption. Similarly, the  $T_{\text{ifree}} / T_{\text{icom.}}$  ratios for 2,6-DM-4-NP complexes are also in the order  $\alpha\text{-MCD-2,6-DM-4-NP} > \alpha\text{-CD-2,6-DM-4-NP}$ . Although the  $K_d$  value for the  $\alpha\text{-MCD-2,6-DM-4-NP}$  complex has not been reported, the results from the  $^1\text{H}$  shift displacements,  $^1\text{H}$  homo- and  $^{15}\text{N-}^1\text{H}$  heteronuclear NOE, and  $^{15}\text{N}$   $T_1$  changes clearly indicate that the orientations of the 2,6-DM-4-NP in the  $\alpha\text{-MCD}$  as well as in the  $\alpha\text{-CD}$  complexes in aqueous solution are similar to those of the 4-NP in such complexes. It can be speculated that the hydrophobic interaction is also the major driving force for the formation of the  $\alpha\text{-MCD-2,6-DM-4-NP}$  inclusion complex.

The  $\alpha$ -MCD forms inclusion complexes with nitrophenols in a manner similar to its parent cyclodextrin in solution. Both the thermodynamic stability and the binding rigidity estimated by  $^{15}\text{N}$   $T_1$  indicate that the host-guest interaction is increased by methylation of the  $\alpha$ -CD.

## CONCLUSION

The  $^1\text{H}$  NMR chemical shifts,  $^1\text{H}$  homonuclear Overhauser effects, and complexation-induced  $^{13}\text{C}$  and  $^{15}\text{N}$  chemical-shift changes have been shown to be useful in determining the structure of cyclodextrin inclusion complexes. However,  $^{15}\text{N}$ - $\{^1\text{H}\}$  NOE and  $^{15}\text{N}$   $T_1$ , which may provide more information about structure and restriction of molecular motion for the guest molecules containing nitrogens, have been less extensively employed. This dissertation demonstrates the usefulness of  $^{15}\text{N}$ - $\{^1\text{H}\}$  NOE and  $^{15}\text{N}$   $T_1$  in the evaluation of the geometry and binding rigidity of cyclodextrin inclusion complexes. Especially, because of the large magnitude of the  $^{15}\text{N}$ - $\{^1\text{H}\}$  heteronuclear NOE enhancement (maximum 400%), compared to that of the  $^1\text{H}$ - $\{^1\text{H}\}$  homonuclear NOE enhancement (maximum 50%), measurement of NOE enhancement for the nitrophenol- $\alpha$ -MCD complexes becomes possible. The  $^{15}\text{N}$ - $\{^1\text{H}\}$  NOE between guest nitrophenols and hosts indicates the nitrophenyl groups are situated inside the cavity for both

$\alpha$ -CD and  $\alpha$ -MCD, suggesting similar modes of binding, although the insertion depth of 2,6-DM-4-NP into the cavity is less than that of 4-NP because of the steric hindrance from the two methyl groups. In addition, the complexation-induced decrease in  $^{15}\text{N } T_1$  can be explained in terms of a complexation-induced increase in binding, which can be related to the stability of the CD-nitrophenol complex in solution. From the changes in the  $^{15}\text{N } T_1$  values, it is concluded that the  $\alpha$ -CD-nitrophenol complexes show weaker binding than the corresponding  $\alpha$ -MCD complexes due to the stronger hydrophobic interaction of  $\alpha$ -MCD with 4-nitrophenols, however, the  $\alpha$ -CD-nitrophenol complexes show stronger binding than the corresponding  $\beta$ -CD complexes due to a larger cavity of  $\beta$ -CD.

## CHAPTER 3 EXPERIMENTAL

### 3.1 Materials

All solvents and reagents were obtained from commercial suppliers and used without further purification unless otherwise noted. N,N-Dimethylformamide (DMF) was distilled from calcium hydride under reduced pressure. Sodium nitrate- $^{15}\text{N}$  ( $\text{Na}^{15}\text{NO}_3$ ) was 99%  $^{15}\text{N}$  enriched. Prior to use, the  $\alpha$ -CD was dried in a vacuum oven at 80 °C for about ten hours and kept in a desiccator with  $\text{P}_2\text{O}_5$ .

### 3.2 General Methods

Melting points were determined on a Thomas Hoover Capillary melting point apparatus. Infrared spectra were recorded on a Perkin-Elmer Spectrum 1000 FT-IR spectrophotometer.  $^1\text{H}$ ,  $^{13}\text{C}$  and  $^{15}\text{N}$  NMR spectra were recorded on Bruker NR300 and NR200 instruments, using  $\text{Me}_4\text{Si}$  for  $^1\text{H}$  and  $^{13}\text{C}$  and a solution of  $^{15}\text{NH}_4^{15}\text{NO}_3$  for  $^{15}\text{N}$  as the external standards.

### 3.3 Synthetic Methods

#### 3.3.1 Synthesis of Permethylated- $\alpha$ -cyclodextrin ( $\alpha$ -MCD)

The synthesis of  $\alpha$ -MCD has been previously reported<sup>64,65,66</sup>. However, experimental details are lacking. Permethylation of  $\alpha$ -CD was carried out in our laboratory using modification of the procedures described by Lehn<sup>64</sup> and Tanimoto.<sup>65</sup>

Dry sodium hydride (1.1g, 45 mmol) and methyl iodide (MeI) (5.7 mL, 90 mmol) were added to a solution of  $\alpha$ -CD (0.485g, 0.50 mmol) in dry DMF (100 mL) under  $N_2$ . The reaction vessel was then protected from exposure to direct lighting and stirred at room temperature for two days, adding 2 additional mL of MeI each day. The excess MeI was then evaporated by stirring the reaction mixture under a slow stream of  $N_2$ . The semisolid mixture of methylated products, obtained after removal of the DMF, was separated by methods A and B.

Method A: The semisolid mixture of methylated products was extracted with chloroform. The chloroform extract were concentrated and the residue was chromatographed on a silica gel 60A column (chloroform-acetone, 9:1) to give yellow crystals of  $\alpha$ -MCD (0.193g, 31.5%), mp 203-204 °C (lit.<sup>66</sup> mp 205 °C) after recrystallization from chloroform-petroleum ether.

Method B: The semisolid mixture of methylated products was extracted with benzene. The benzene extract was concentrated and the residue was separated on an activated carbon column with benzene as the eluent to give yellowish crystalline  $\alpha$ -MCD (0.24g 40%), mp 203-204 °C (lit.<sup>64</sup> mp 205 °C) after recrystallization from chloroform-petroleum ether. The complete methylation of  $\alpha$ -MCD was confirmed by the absence of hydroxyl stretching in the IR spectrum (KBr) of  $\alpha$ -CD (Figure 20), and the appearance of -OCH<sub>3</sub> signals at  $\delta$ 3.64, 3.52 and 3.41 in the <sup>1</sup>H NMR spectrum and at  $\delta$ 57.84, 58.93 and 61.74 in the <sup>13</sup>C NMR spectrum (Figure 21). Also, the signals for the six skeletal carbons at  $\delta$ 71.21, 71.46, 81.25, 82.21, 82.45 and 100.09 confirmed the symmetry of the molecule. These results are consistent with those reported by Lehn.<sup>64</sup>

### 3.3.2 Synthesis of 4-Nitrophenol-<sup>15</sup>N (4-NP-<sup>15</sup>N)

A mixture of 1.4 mL (2.5 g) of concentrated sulfuric acid, 4.0 mL of water, and 1.0 g ( $1.16 \times 10^{-2}$  mmol) of Na<sup>15</sup>NO<sub>3</sub> was cooled to 0 °C in an ice bath. Phenol (0.94 g, 10.0 mmol) was added to the mixture at such a rate that the temperature did not rise above 20 °C. The solution was stirred for one hour after all the phenol had been added. The reaction mixture was filtered with suction to give a mixture of *para*- and *ortho*- nitrophenols which was dissolved in methylene chloride (20 mL). The methylene

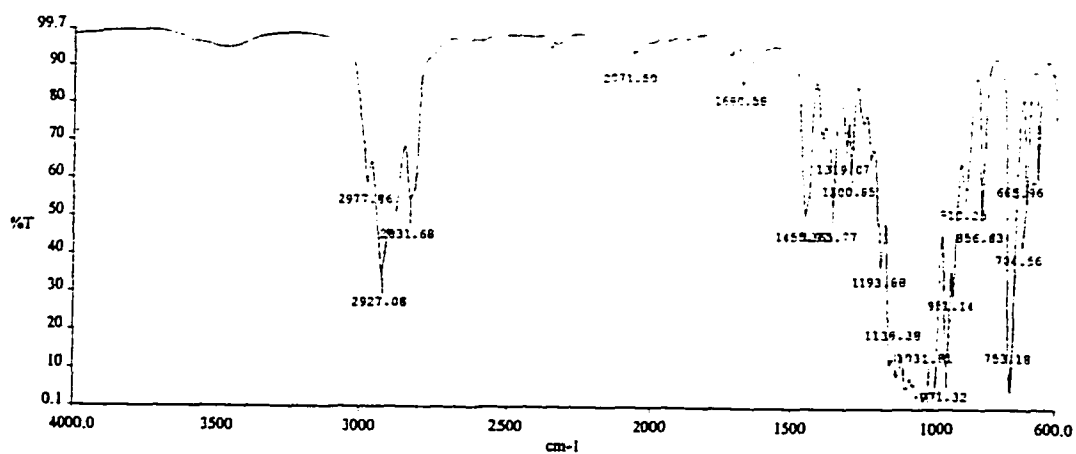
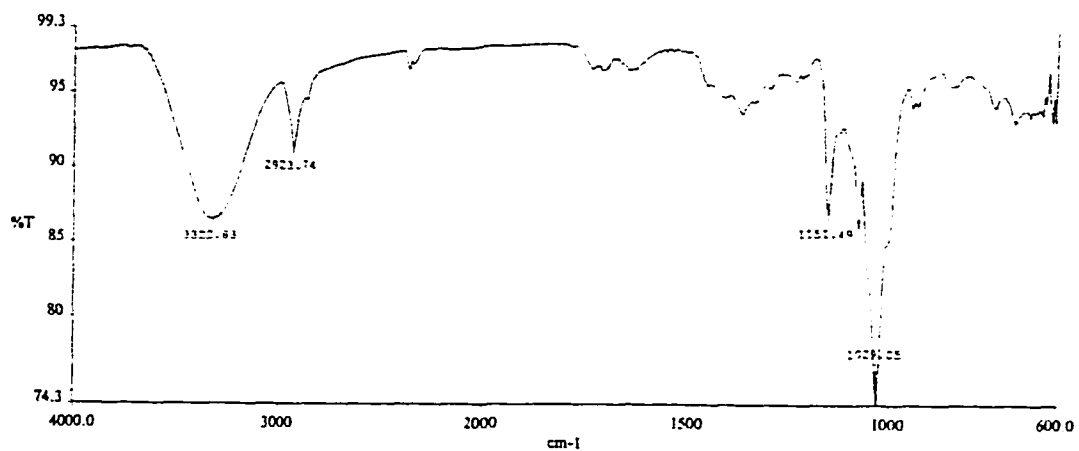
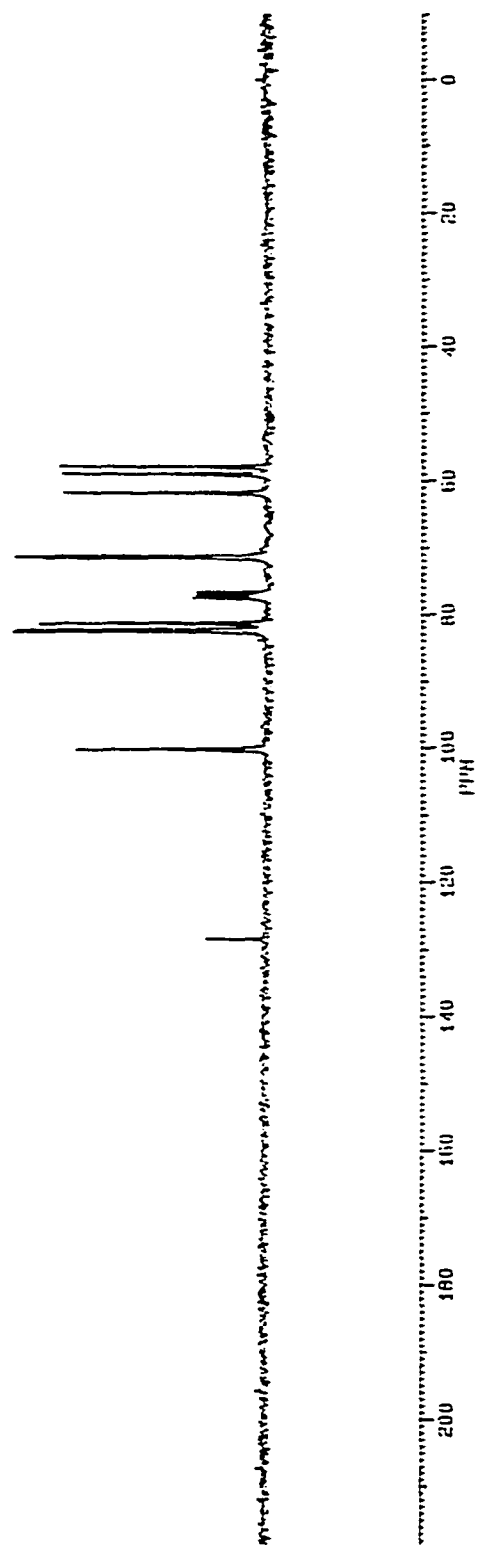


Figure 20. IR spectra of  $\alpha$ -CD (top) and  $\alpha$ -MCD (bottom) measured in KBr pellet.



**Figure 21.** 75 MHz  $^{13}\text{C}$  spectrum of  $\alpha$ -MCD in  $\text{CDCl}_3$ .

chloride solution was washed with water (2 x 15 mL), dried over  $\text{MgSO}_4$ , filtered and concentrated in vacuo. The residue was chromatographed on alumina, eluting first with methylene chloride to remove the ortho isomer and then with ether:methanol (1:1) to elute the para isomer. The yield of yellow crystalline 4-nitrophenol- $^{15}\text{N}$  was 0.23 g (18.5%): mp 112-113 °C (lit.<sup>67</sup> mp 113-115 °C):  $^1\text{H NMR}$   $\delta$  8.05 (d, 2H), 6.67 (d, 2H).

### 3.3.3 Synthesis of 2,6-Dimethyl-4-nitrophenol- $\text{N}^{15}$ (2,6-DM-4-NP- $^{15}\text{N}$ )

The nitration of 2,6-dimethylphenol was carried out by a modification of the procedure reported by Gaude.<sup>67</sup> The 2,6-dimethylphenol (0.40g, 3.27 mmol) was added to a mixture of diethyl ether (6.6 mL), water (6.6 mL) and sodium nitrate- $^{15}\text{N}$  (0.40 g, 4.65 mmol), and then HCl (2 mL, 11 N) was added. The mixture was stirred at room temperature for four days, and the red precipitate formed was collected by filtration and washed with a 50% methanol aqueous solution. Evaporation of the methanol solution gave the crude product. Additional crude product was obtained by extracting the filtrate three times with diethyl ether, washing the extracts to neutrality, drying over sodium sulfate and concentrating in vacuo. The combined crude products were recrystallized from methanol-water to give yellow crystalline 2,6-

dimethyl-4-nitrophenol (0.25g, 46%): mp 168 °C (lit.<sup>67</sup> mp 168 °C); <sup>1</sup>H NMR δ 8.29 (s, 2H), 2.21 (s, 6H).

### 3.4 NMR Methods

#### 3.4.1 Sample Preparation

All NMR samples were prepared in a buffer solution made up with anhydrous Na<sub>2</sub>HPO<sub>4</sub> in D<sub>2</sub>O, and the pD was adjusted to 11 with a solution of 0.1 N NaOD in deuterium oxide. The cyclodextrin hydroxyl protons were exchanged for deuterium by lyophilizing 1g of the cyclodextrins from 80 mL of D<sub>2</sub>O three times.

#### 3.4.2 NMR Spectroscopy

All structural determinations of inclusion complexes by <sup>1</sup>H NMR were recorded on Bruker NR 300 and NR 200 spectrometers with 16 K computer memory over a spectral width of 3300 Hz and 2200 Hz, respectively. The concentrations of 4-nitrophenols and cyclodextrins were 0.03M and 0.01M, respectively in an alkaline buffer solution (pD11). No internal <sup>1</sup>H NMR reference was added since the possibility of the reference

molecule binding to the cyclodextrins could not be excluded. Shifts are reported in ppm ( $\delta$ ) relative to an external capillary of 1% TMS in  $\text{CDCl}_3$ .

Proton-decoupled  $^{13}\text{C}$  NMR spectra were recorded at 75 MHz. A pulse width of 5.5  $\mu\text{sec}$  ( $90^\circ$ ) and a pulse delay of 6~10 seconds were utilized because of the long relaxation time ( $T_1$ ) of the quaternary carbons in the substrate. The concentrations of 4-nitrophenols and cyclodextrins were 0.033M and 0.050M, respectively in an alkaline buffer solution (pD11). Based on the dissociation constants ( $K_d$ 's) for  $\alpha$ -CD ( $6.1 \times 10^{-4}$  M) and  $\beta$ -CD ( $1.5 \times 10^{-3}$  M), it was estimated that 4-NP in the presence of  $\alpha$ -CD and  $\beta$ -CD was 99% and 80% bound, respectively.<sup>31,49</sup>

The  $^{15}\text{N}$  NMR spectra were recorded at 20 MHz, using a 10 mm probe with inverse gated decoupling, a pulse angle of  $90^\circ$  and an acquisition time of 0.5 s with 6~10 s recycle delay for 4 K data points over a spectral width of 4065 Hz. Nitrogen chemical shifts are reported with respect to saturated  $^{15}\text{NH}_4^{15}\text{NO}_3$  (99%  $^{15}\text{N}$  atom enrichment) as an external reference with 20.68 ppm for  $^{15}\text{NH}_4^-$  and 376.25 ppm for  $^{15}\text{NO}_3^-$ .<sup>55</sup>

### 3.4.3 $^{15}\text{N}$ - $\{^1\text{H}\}$ Heteronuclear Overhauser Enhancements

To obtain the heteronuclear NOE difference spectra, the intermolecular heteronuclear NMR experiments were measured under the computer control of an Aspect 3000 system. For the NMR samples,

0.025M solutions of 4-NP and 2,6-DM-4-NP, and 0.0375M solutions of  $\alpha$ -CD and  $\alpha$ -MCD were used. All data were acquired under temperature control at 30 °C. Prior to the 90°  $^{15}\text{N}$  observe pulse, the  $^1\text{H}$  decoupler was set on one of the hydrogen resonances, which was saturated long enough to build up heteronuclear NOE at the nitrogen. Using a 10 mm probe, satisfactory results were achieved by setting the decoupler power level to 0.10-0.12 watt for an irradiation time of 75-125 seconds. The data were acquired either with the decoupler gated off, or under broad band decoupling with the decoupling frequency set to the center of the  $^1\text{H}$  region. Steady-state conditions were used for a build-up of NOE. Therefore, the acquisition time was chosen to be as short as was compatible with the desired digital resolution and the spectral width was reduced to the region of interest. Data were taken by alternating the frequency for the proton decoupler between on- and off-resonance. To obtain the difference spectra, the off-resonance data accumulated with the  $^1\text{H}$  decoupler set at the down-field end of the  $^1\text{H}$  NMR range were subtracted from the on-resonance data. An exponential line broadening (LB) of 3 Hz was performed before transformation of the FID. Eighty transients were accumulated in each case in order to obtain a good signal-to-noise ratio.  $^1\text{H}$  NMR spectra were obtained with the same instrument but with a different probe (5 mm probe) to determine the decoupler positions.

#### 3.4.4 Determination of $^{15}\text{N}$ Spin-lattice Relaxation Times

$^{15}\text{N}$  spin-lattice relaxation times were measured by the inversion-recovery method using a  $180^\circ$ - $t_1$ - $90^\circ$ - $t_2$  pulse sequence, where  $t_1$  is the time in seconds between the  $180^\circ$  and  $90^\circ$  pulses and  $t_2$ , the waiting time between pulses, was equal to at least  $5T_1$ . The spin-lattice relaxation time,  $T_1$ , was then determined from a least-squares fit of signal intensities and  $t$  values in the expression  $M_t = M_\infty[1-(2\exp(-t/T_1))]$ , where  $M_t$  is the magnetization measured at the time  $t$ . The estimated error in  $T_1$  was less than  $\pm 5\%$  in three consecutive experiments. For the NMR samples, 0.025M solutions of 4-nitrophenols and 0.0375M solutions of cyclodextrins were used. Samples were deoxygenated with nitrogen in order to prevent the paramagnetic effect on  $T_1$  values from oxygen molecules. The temperature was kept at  $30^\circ\text{C}$  for all experiments.

#### 3.4.5 $^1\text{H}$ - $^1\text{H}$ COSY Experiments

The COSY experiments were performed using the standard automation microprograms provided with the Bruker Aspect 3000 data system. The pulse sequence is as follows: delay- $90^\circ$ - $t_1$ - $45^\circ$ - $t_2$ , where  $t_1$  is an incremented delay and  $t_2$  is the acquisition time. A typical proton-proton

correlated spectrum was acquired with spectral width in  $f_1$  and  $f_2$  of 750 Hz at 300 MHz. The spectra were acquired with 512w data points in the  $f_1$  and  $f_2$  domain and 8 transients (two dummy scans) over 128 experiments. The delay between scans was 1.5 seconds. A sine-bell multiplication was applied to both dimensions.

#### 3.4.6 NOESY experiments

The NOESY spectra were obtained on a Bruker NR 300 by using the standard pulse sequence<sup>62</sup> as follows:  $\pi/2-t_1-\pi/2-\tau-\pi/2$ -Acquire. For each  $t_1$  value, 8 transients for both the 4-NP and 2,6-DM-4-NP systems were signal-averaged with a pulse delay of 1.5 seconds and a mixing time of 500 ms. The 256 free-induction decays were acquired with 1k data points and a spectral width of 1650 Hz for the  $\alpha$ -MCD complex with 4-NP and 1930 Hz for the  $\alpha$ -MCD complex with 2,6-DM-4-NP. The data matrix was multiplied with sine bell window functions in both dimensions.

## APPENDIX A

### ASSIGNMENT OF THE $^1\text{H}$ , $^{13}\text{C}$ AND $^{15}\text{N}$ RESONANCES IN CYCLODEXTRIN NITRATES BY 2D NMR AND THE DETERMINATION OF THE REGIOSELECTIVITY OF THE HYDROXYLAMINE-INDUCED DENITRATION REACTIONS

Crystalline  $\alpha$ - and  $\beta$ -cyclodextrin nitrates with a degree of substitution less than 3 have previously been prepared by the reaction of the cyclodextrin with nitrogen pentoxide in chloroform in the presence of sodium fluoride.<sup>68</sup> Other examples of the preparation of polynitrated cyclodextrins appear in the literature, but the elemental analysis results are generally inconsistent [the theoretical value is 14.1% for  $(\text{C}_6\text{H}_7\text{O}_{11}\text{N}_3)_n$ ] with the formation of completely<sup>69</sup> or partially<sup>70</sup> nitrated materials. In more recent work,<sup>71</sup> the presence of OH stretching bands in the IR spectra of prepared nitrate derivatives of cyclodextrins suggested that a small number of hydroxyl groups had not been nitrated.

In our laboratory isotopomeric ( $^{14}\text{N}$  and  $^{15}\text{N}$ ) materials were prepared by the reaction of  $\alpha$ - and  $\beta$ -cyclodextrin with 100% nitric acid in the presence of phosphorus pentoxide, as previously describes for the preparation of amylose trinitrate.<sup>72</sup> While the nitrogen content of these

$\alpha$ - and  $\beta$ -cyclodextrin nitrate derivatives was found to be slightly low (13.5%), the mass spectra exhibited molecular ions corresponding to complete conversion to  $C_{36}H_{42}O_{66}N_{18}$  and  $C_{42}H_{49}O_{77}N_{21}$  ( $m/z$  1782 and 2079 respectively). Despite rigorous drying efforts, there was indication of possibly incavitated water being retained by these samples, leading to poor elemental analyses. This was confirmed by the appearance of a water signal in the proton NMR spectra of these materials measured in anhydrous acetone- $d_6$ . That these compounds were essentially completely nitrated was further indicated by the presence of only six carbon resonances in their  $^{13}C$  NMR spectra. Illustrated for heptakis(2,3,6-tri-*O*-nitro)- $\beta$ -cyclodextrin in Figs 22, 23 and 24 are typical spectra, the homonuclear shift correlated spectrum and one-bond  $^{13}C$ - $^1H$  and three-bond  $^{15}N$ - $O$ - $^1H$  heteronuclear shift correlated spectra, from which unequivocal assignment of all nuclei can be deduced. These correlated chemical shift data for  $\alpha$ - and  $\beta$ -cyclodextrins and their corresponding fully nitrated derivatives, hexakis(2,3,6-tri-*O*-nitro)- $\alpha$ -cyclodextrin and heptakis(2,3,6-tri-*O*-nitro)- $\beta$ -cyclodextrin, measured in DMSO- $d_6$  are summarized in Table X. The assignment of C-6 was independently confirmed by a DEPT experiment.

As has been previously noted, the resonance signals of C-1 and C-2 in nitrates exhibit a considerable down field shift and upfield shift, respectively, compared with the alcohols from which they are derived. The

**Table X. Correlated  $^1\text{H}$ ,  $^{13}\text{C}$  and  $^{15}\text{N}$  Chemical Shifts (ppm) for  $\alpha$ - and  $\beta$ -Cyclodextrins and Their Corresponding Fully Nitrated Derivatives, Hexakis(2,3,6-tri-*O*-nitro)- $\alpha$ -cyclodextrin and Heptakis(2,3,6-tri-*O*-nitro)- $\beta$ -cyclodextrin, Measured in  $\text{DMSO-}d_6$**

<u><math>\alpha</math>-cyclodextrin</u>			<u>Hexakis(2,3,6-tri-<i>O</i>-nitro)-<math>\alpha</math>-cyclodextrin</u>				
$\delta^1\text{H}$	$\delta^{13}\text{C}$		$\delta^1\text{H}$	$\delta^{13}\text{C}$		$\delta^{15}\text{N}^a$	
H-1 4.83	C-1 102.03		H-1 5.69	C-1 97.66			
H-2 3.26	C-2 72.15		H-2 5.42	C-2 76.28	N-2	331.7	
H-3 3.78	C-3 73.31		H-3 5.43	C-3 76.92	N-3	333.60	
H-4 3.43	C-4 82.12		H-4 4.52	C-4 77.45			
H-5 3.62	C-5 72.15		H-5 4.33	C-5 68.98			
H-6 3.67	C-6 60.04		H-6 4.85	C-6 70.91	N-6	337.64	
<u><math>\beta</math>-cyclodextrin</u>			<u>Heptakis(2,3,6-tri-<i>O</i>-nitro)-<math>\beta</math>-cyclodextrin</u>				
H-1 4.81	C-1 102.00		H-1 5.60	C-1 97.90			
H-2 3.29	C-2 72.47		H-2 5.50	C-2 76.01	N-2	331.69	
H-3 3.65	C-3 73.12		H-3 5.33	C-3 77.06	N-3	333.50	
H-4 3.36	C-4 81.61		H-4 4.47	C-4 77.06			
H-5 3.54	C-5 72.10		H-5 4.20	C-5 68.96			
H-6 3.55	C-6 59.99		H-6 4.85	C-6 70.80	N-6	337.50	
	3.64			4.95			

<sup>a</sup> Measured against external  $\text{NaNO}_3$  (saturated solution) at  $\delta$  376.53 ppm

magnitude of these observed  $\beta$  and  $\gamma$  shifts due to the incorporation of nitrate ester functions in the cyclodextrins are consistent with the empirical predictions that have been developed.<sup>73</sup> The greatest downfield shift (*ca.* 11 ppm) is experienced by C-6, which has no adjacent carbons bearing a nitrate group, whereas C-2 and C-3, each with one neighboring  $\text{ONO}_2$  group, are shifted downfield to a lesser extent (*ca.* 4 ppm). All other carbons are shifted upfield. The assignment of the nitrogen resonances was advantageously achieved by means of the small (*ca.* 4 Hz) three-bond  $^{15}\text{N}$ -O-C- $^1\text{H}$  spin coupling that exists,<sup>72,74</sup> which made the heteronuclear correlation possible.

### **Denitration of Hexakis(2,3,6-tri-*O*-nitro)- $\alpha$ -cyclodextrin and Heptakis(2,3,6-tri-*O*-nitro)- $\beta$ -cyclodextrin**

Treatment of either hexakis(2,3,6-tri-*O*-nitro)- $\alpha$ -cyclodextrin or heptakis(2,3,6-tri-*O*-nitro)- $\beta$ -cyclodextrin with an excess of freshly prepared hydroxylamine in anhydrous pyridine evolved bubbles of nitrogen continuously for about 24 h at room temperature. The progress of the reaction could easily be monitored by either  $^1\text{H}$ ,  $^{13}\text{C}$  or  $^{15}\text{N}$  NMR and at the end of this period the reaction was judged to be complete. Quenching the reaction in water gave rise in each case to a crystalline product. For the reaction involving heptakis(2,3,6-tri-*O*-nitro)- $\beta$ -cyclodextrin the  $^{15}\text{N}$

spectra of the starting material and products are illustrated in Fig. 25. It is clear from these spectra that the starting material, which exhibits three  $^{15}\text{N}$  resonances signals, has been converted to a new material showing only two  $^{15}\text{N}$  resonance signals, implying the selective removal of one of the nitrate functions. Although the one-bond  $^{13}\text{C}$ - $^1\text{H}$  heteronuclear shift correlation spectrum could readily be obtained, attempts to measure the three-bond  $^{15}\text{N}$ -O-C- $^1\text{H}$  shift correlation spectrum in the denitrated products were unsuccessful, and we tentatively attribute this failure to  $J$  (ca. 4 Hz) being less than  $1/T_2$ . Nonetheless, the  $^1\text{H}$ ,  $^{13}\text{C}$  and  $^{15}\text{N}$  chemical shift assignments and the structure for these denitrated materials could be deduced.

The  $^{15}\text{N}$  spectrum obtained by gating the decoupler showed a doublet at  $\delta$  337.59 ( $J = 3.9$  Hz) and a broad signal at  $\delta$  338.74 (overlapping doublets), which could be assigned to nitrogen atoms at position 3 and 6, respectively. These assignments, summarized in Table XI, could be confirmed by diagnostic changes that have previously been observed in the chemical shifts exhibited by atoms neighboring the reaction site in related nitration/denitration reactions.<sup>72</sup> Thus, denitration, in effect the replacement of an  $\text{NO}_2$  group by H, converts the nitrate ester to the hydroxyl function. This change is expected to bring about a substantial upfield shift of the carbinol carbon (ca. 7-10 ppm) and a downfield shift (ca. 4 ppm) of the nitrate- $^{15}\text{N}$  resonance flanking the newly introduced OH group. The selective denitration at position 2 is consistent with these

observations: C-2 is shifted upfield by 8.4 ppm and N-3 downfield by 4.1 ppm. Other nitrate-<sup>15</sup>N resonances, more remote from the denitration site, e.g. N-6, experience a downfield shift but to a lesser extent (*ca.* 1-2 ppm), whereas carbon resonances are substantially unchanged or, in the case of the flanking C-1 and C-3, are shifted downfield (*ca.* 4 ppm).

**Table XI. Correlated  $^1\text{H}$ ,  $^{13}\text{C}$  and  $^{15}\text{N}$  Chemical Shifts (ppm) Measured in  $\text{DMSO-}d_6$  for Denitration products, Hexakis(3,6-di-*O*-nitro)- $\alpha$ -cyclodextrin and Heptakis(3,6-di-*O*-nitro)- $\beta$ -cyclodextrin, Resulting from Reactions of Hexakis(2,3,6-tri-*O*-nitro)- $\alpha$ -cyclodextrin and Heptakis(2,3,6-tri-*O*-nitro)- $\beta$ -cyclodextrin with Hydroxylamine in Pyridine**

Hexakis(3,6-di- <i>O</i> -nitro)- $\alpha$ -cyclodextrin							
	$\delta$ $^1\text{H}$		$\delta$ $^{13}\text{C}$	$\Delta^a$		$\delta$ $^{15}\text{N}^b$	$\Delta^c$
H-1	5.00	C-1	101.66	(+4.0)			
H-2	3.55	C-2	67.67	(-8.6)	N-2	—	
H-3	5.48	C-3	81.58	(+4.7)	N-3	337.94	(+4.4)
H-4	3.92	C-4	78.54	(+1.1)			
H-5	4.33	C-5	68.50	(-0.5)			
H-6	4.95	C-6	71.85	(+0.9)	N-6	338.90	(+1.3)

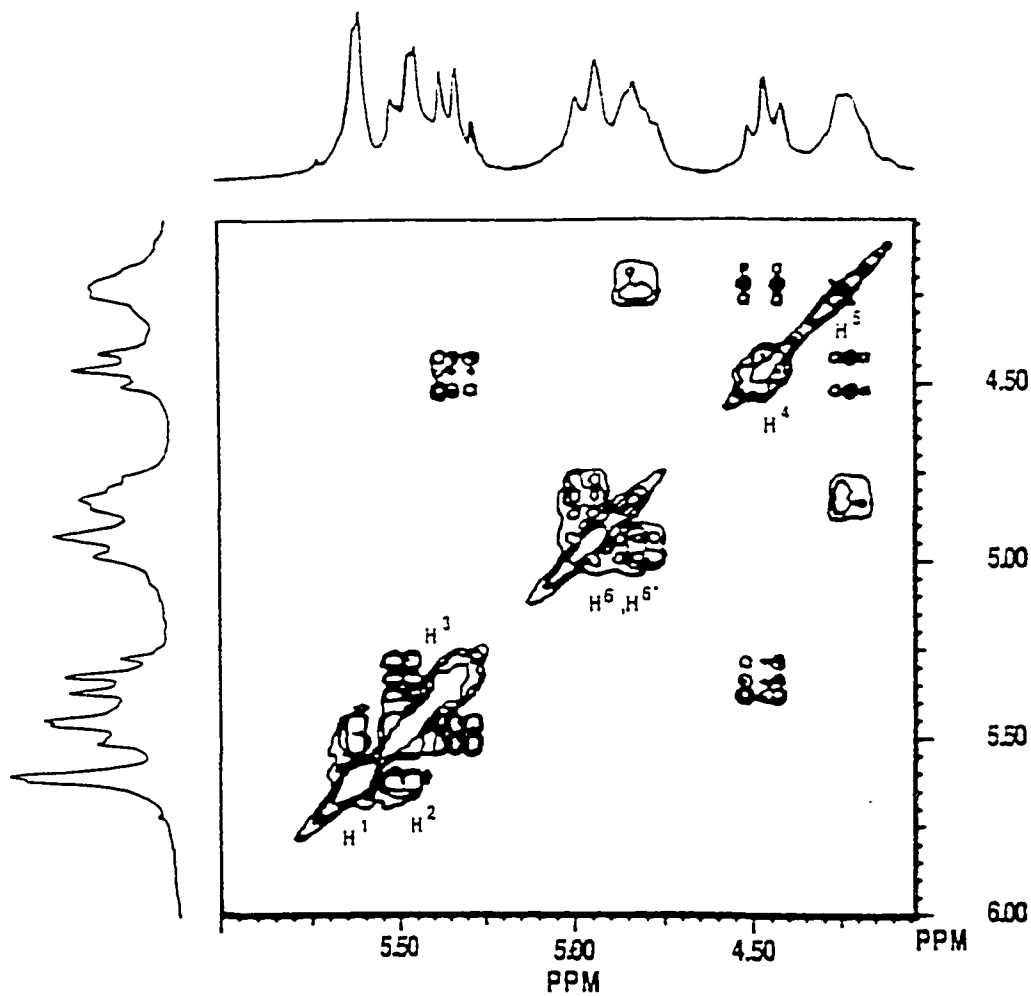
  

Heptakis(3,6-di- <i>O</i> -nitro)- $\beta$ -cyclodextrin							
	$\delta$ $^1\text{H}$		$\delta$ $^{13}\text{C}$	$\Delta^a$		$\delta$ $^{15}\text{N}^b$	$\Delta^c$
H-1	5.00	C-1	101.81	(+3.9)			
H-2	3.51	C-2	67.74	(-8.4)	N-2	—	
H-3	5.22	C-3	81.34	(+4.3)	N-3	337.59	(+4.1)
H-4	3.85	C-4	78.19	(+1.1)			
H-5	4.20	C-5	68.51	(-0.5)			
H-6	4.94	C-6	71.55	(+0.8)	N-6	338.74	(+1.2)

<sup>a</sup>  $\delta$   $^{13}\text{C}$  (denitration product) -  $\delta$   $^{13}\text{C}$  (nitrate starting material); positive values correspond to downfield shift.

<sup>b</sup> Measured against external  $\text{NaNO}_3$  (saturated solution) at  $\delta$  376.53 ppm.

<sup>c</sup>  $\delta$   $^{15}\text{N}$  (denitration product) -  $\delta$   $^{15}\text{N}$  (nitrate starting material); positive values correspond to downfield shift.



**Figure 22.** Contour plot of 300 MHz COSY 90 spectrum of heptakis(2,3,6-tri-*O*-nitro)- $\beta$ -cyclodextrin measured in DMSO-*d*<sub>6</sub>.

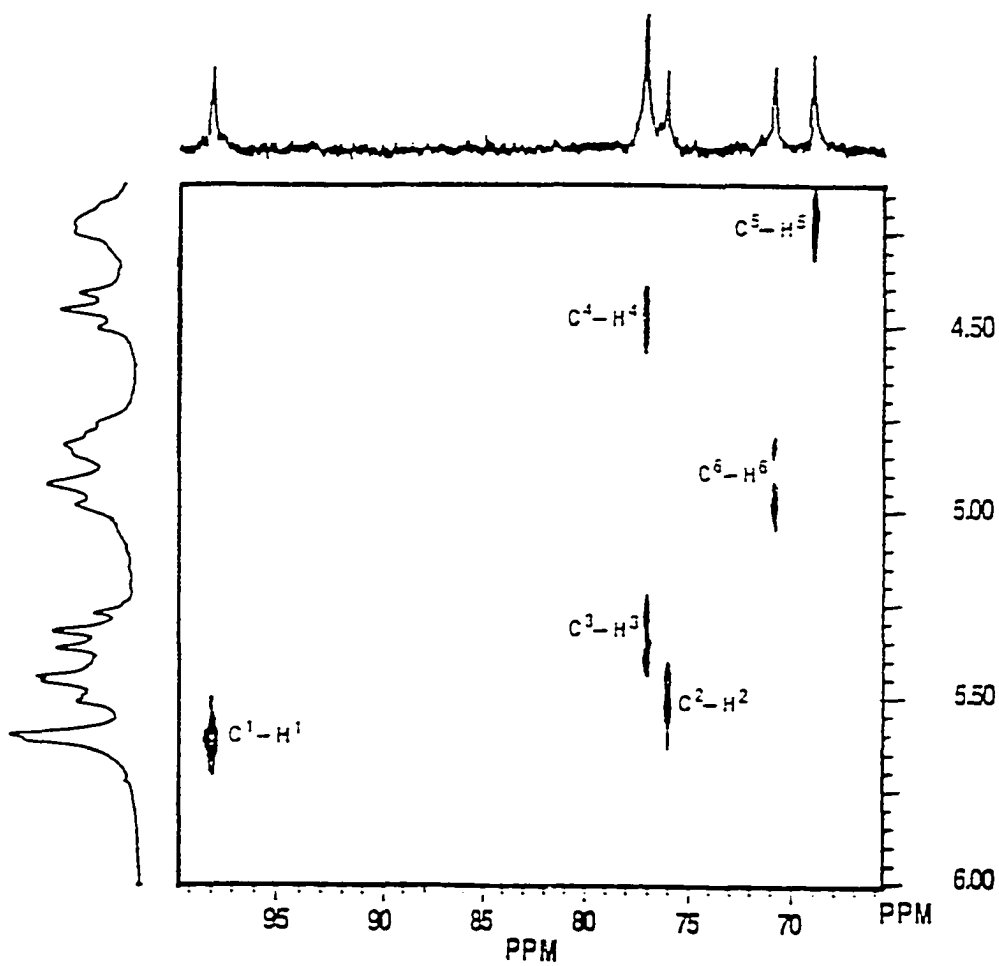
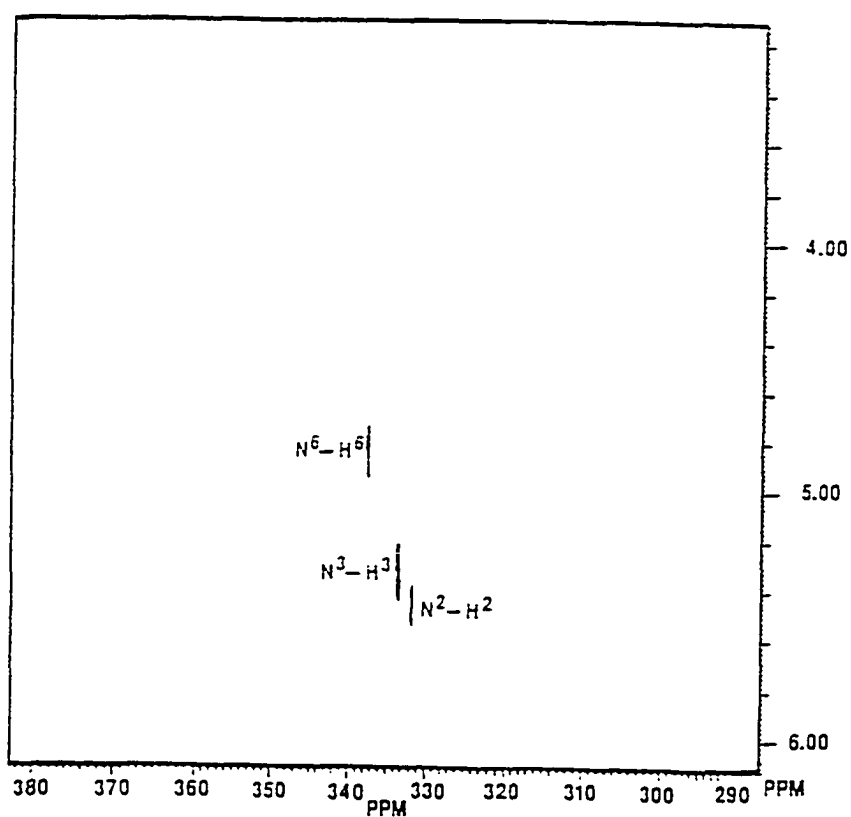
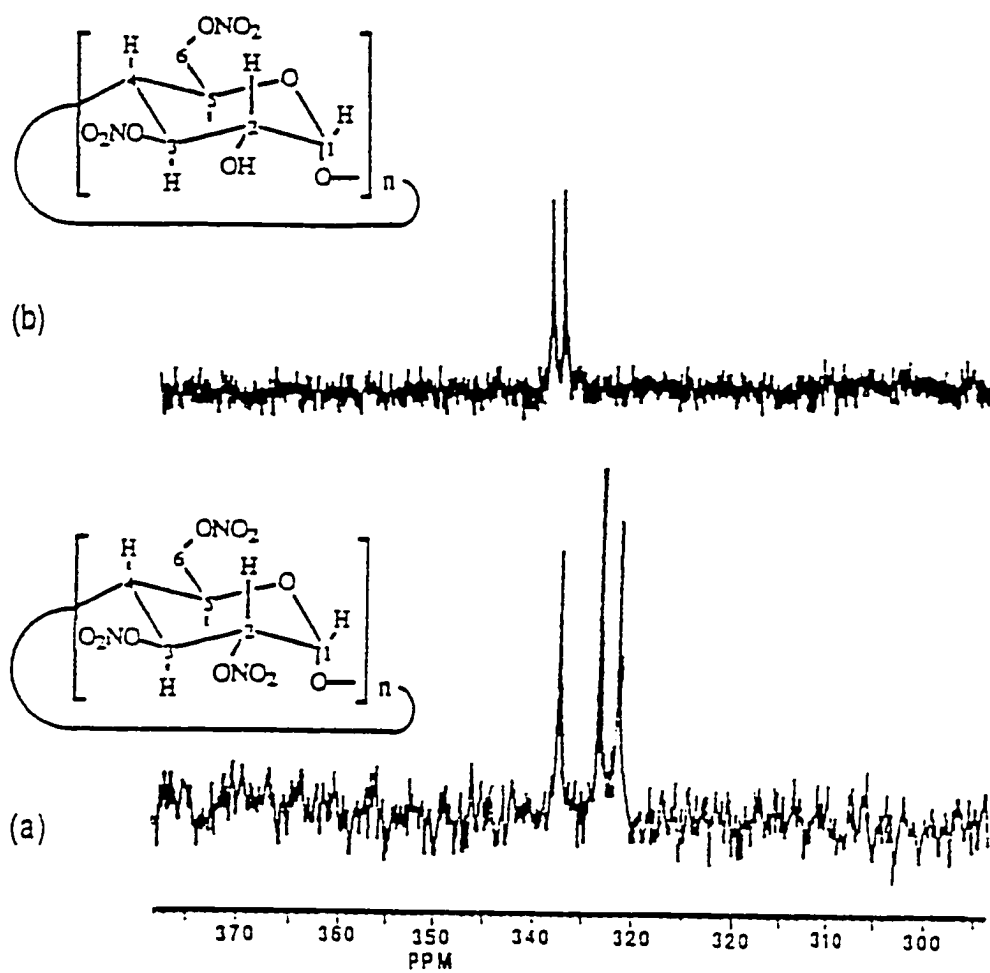


Figure 23. Contour plot of the  $^{13}\text{C}$ - $^1\text{H}$  correlated spectrum of heptakis(2,3,6-tri-*O*-nitro)- $\beta$ -cyclodextrin measured in  $\text{DMSO-}d_6$



**Figure 24.** Contour plot of the  $^{15}\text{N}$ -O-C- $^1\text{H}$  correlated spectrum of heptakis(2,3,6-tri-*O*-nitro)- $\beta$ -cyclodextrin measured in  $\text{DMSO-}d_6$



**Figure 25.** Comparison of 20 MHz  $^{15}\text{N}$  spectra measured in  $\text{DMSO-}d_6$  of (a) heptakis(2,3,6-tri-*O*-nitro)- $\beta$ -cyclodextrin- $^{15}\text{N}_{21}$  and (b) its denitration product, heptakis(3,6-di-*O*-nitro)- $\beta$ -cyclodextrin- $^{15}\text{N}_{14}$ , from reaction with hydroxylamine in pyridine.

## References

- (1) Demarco, P. V.; Thakkar, A. L. *J. Chem. Soc. Chem. Commun.* **1970**, 2.
- (2) Duchene, D.; Wouessidjewe, D. *J. Coord. Chem.* **1992**, 27, 223.
- (3) Inoue, Y. *NMR Studies of Structure and Properties of Cyclodextrins and Their Inclusion Complexes, Annual Reports on NMR Spectroscopy*; Academic Press: 1993; Vol. 27, p 59.
- (4) Villiers, A. C. *R. Acad. Sci.* **1891**, 112, 536.
- (5) Schardinger, F. *Wien. Klin. Wochenschr.* **1904**, 17, 207.
- (6) French, D.; Pulley, A. O.; Effenberger, J. A.; Rougrie, M. A.; Abdullah, M. *Arch. Biochem. Biophys.* **1965**, 111, 153.
- (7) Pulley, A. O.; French, D. *Biochem. Biophys. Res. Commun.* **1961**, 5, 11.
- (8) Szejtli, J. *Compr. Supramol. Chem.* Elsevier: Oxford, UK 3 , 6, 1996.
- (9) French, D. *Adv. Carbohydr. Chem.* **1957**, 12, 189.
- (10) Sundararajan, P. R.; Rao, V. S. R. *Carbohydrate Res.* **1970**, 13, 351.
- (11) Nakagawa, T.; Ueno, K.; Kashiwa, M.; Watanabe, J. *Proceedings of the 7th International Symposium on Cyclodextrins, Tokyo*, ed. Osa, T. Publ. Office Acad. Soc. Japan, Tokyo, 1994; p 114.

- (12) Endo, T.; Ueda, H.; Kobayashi, S.; Nagai, T. Proceedings of the 7th International Symposium on Cyclodextrins, Tokyo. ed. Osa, T. Publ. Office Acad. Soc. Japan, Tokyo, 1994; p.66.
- (13) Saenger, W. *Inclusion Compounds II* edited by Atwood, J. L.; Davis, J. E. D.; MacNicol, D. D. Academic Press: London, 1984; p 231.
- (14) Bergeron, R. J. *Inclusion Compounds III*. edited by Atwood, J. L.; Davis, J. E. D.; MacNicol, D. D. Academic Press: London, 1984; p 391.
- (15) Li, S.; Purdy, W. C. *Chem. Rev.* **1992**, 92, 1457.
- (16) Takeo, K.; Kuge, T. *Agric. Biol. Chem.* **1970**, 34, 1787.
- (17) Gillet, B.; Nicol, D. J.; Delpuech, J. J. *Tetrahedron Lett.* **1982**, 23, 65.
- (18) Ress, D. A. *J. Chem. Soc.* **1970**, (B), 877.
- (19) Schonberger, B. P.; Jansen, A. C. A.; Janssen, L. H. M. Proceedings of the 4th International Symposium on Cyclodextrins, Munich, 1988, eds. Huber, O.; Szejtli, J. Kluwer, Dordrecht, 1988, p.61.
- (20) Duchene, D. (ed.) *New Trends in Cyclodextrins and Derivatives* Editions de Sante, Paris, 1991.
- (21) Szejtli, J. (ed) *Cyclodextrin Technology* Kluwer Academic, Dordrecht, The Netherlands, 1988.
- (22) Desire, B.; Saint-Andre, S. *Fundam. Appl. Toxicol.* **1986**, 7(4), 646.

- (23) Fukazawa, T.; Futase, T. *Jpn. Kokai JP 90268 643*, **1990**.
- (24) Uekama, K.; Irie, T. *Compr. Supramol. Chem.* Elsevier: Oxford, UK 3, 451, **1996**.
- (25) Uekama, K.; Hirayama, F.; Irie, T. *High performance Biomaterials. A Comprehensive Guide to Medical and Pharmaceutical Applications*: Technomic Publishing Co. Inc.: Lancaster, PA, 1991; p 789.
- (26) Uekama, K.; Horiuchi, Y.; Irie, T. Hirayama, F. *Carbohydr. Res.* **1989**, 192, 323.
- (27) Szejtli, J. *J. Inclusion Phenom.* **1983**, 1, 135.
- (28) Brewster, M. E.; Simpkins, J. W.; Hora, M. S.; Stern, W. C.; Bodor, N. *J. Parenter. Sci. Technol.* **1989**, 43, 231.
- (29) Yamamoto, M.; Yoshida, A.; Hirayama, F.; Uekama, K. *Int. J. Pharm.* **1989**, 49, 183.
- (30) Hirayama, F. *Yakugaku Zasshi.* **1993**, 113, 425.
- (31) Inoue, Y.; Takahashi, Y.; Chujo, R. *Carbohydr. Res.* **1985**, 144, C9.
- (32) Saenger, W. *Angew. Chem. Int. Ed. Engl.* **1980**, 19, 344.
- (33) Szejtli, J. *Cyclodextrin Technology*; Kluwer, Dordrecht, **1988**.
- (34) Nag, A.; Kundu, T.; Bhattacharyya, K. *Chem. Phys. Lett.* **1989**, 157, 83.
- (35) Bergeron, R. J.; Rowar, R. *Bioorg. Chem.* **1976**, 5, 425.

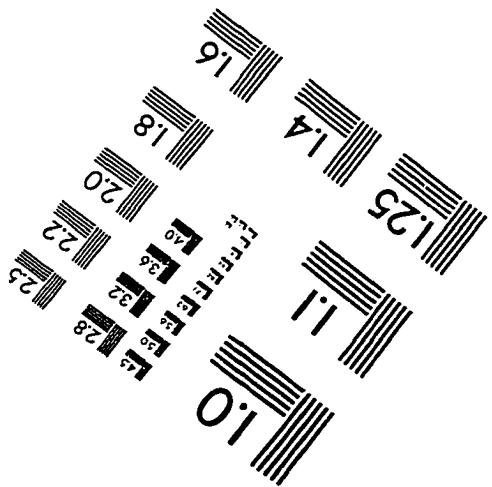
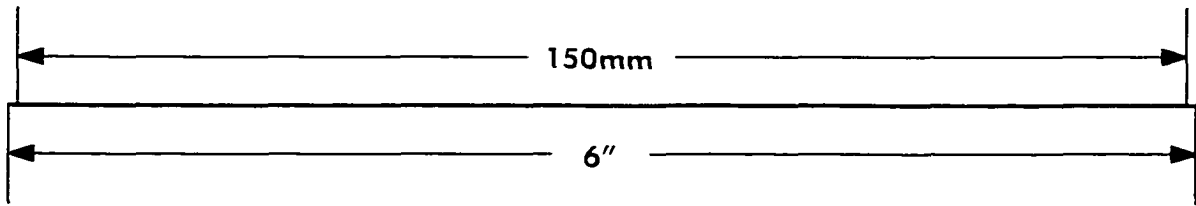
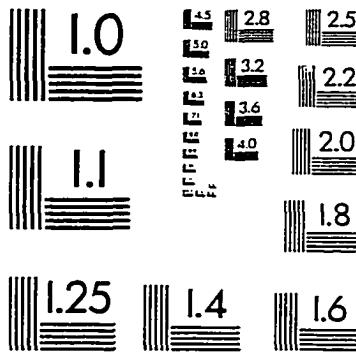
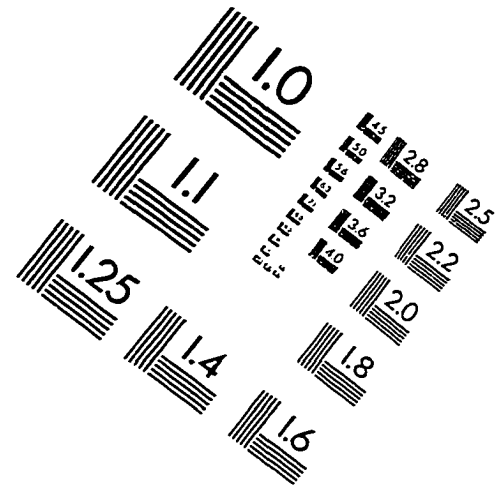
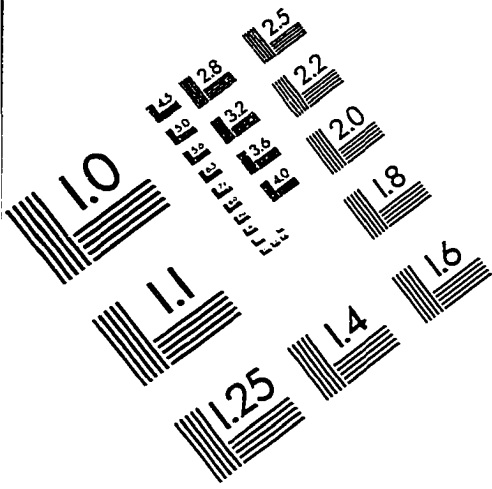
- (36) Kover, K. E.; Batta, G. *Progress in NMR Spectroscopy* **1987**, *19*, 223.
- (37) Levy, G. C.; Cargioli, J. D.; Anet, F. A. L. *J. Am. Chem. Soc.* **1973**, *95*, 1527.
- (38) Rahmm, A. *Nuclear Magnetic Resonance*; Springer-Verlag: New York, 1986: p 126.
- (39) Bovey, F. A. *Nuclear Magnetic Resonance Spectroscopy* : Academic Press, Inc.: San Diego, 2nd Ed., 1988: p 261.
- (40) Solomon, I. *Phys. Rev.* **1955**, *99*, 559.
- (41) Vold, R. L.; Waugh, J. S.; Klein, M. P.; Phelps, D. E. *J. Chem. Phys.* **1968**, *48*, 3831.
- (42) Kuhlmann, K. F.; Grant, D. M.; Harris, R. K. *J. Chem. Phys.* **1968**, *48*, 3831.
- (43) Noggle, J. H.; Schirmer, R.E. *The Nuclear Overhauser Effect-Chemical Applications*; Academic Press: New York, 1971.
- (44) Ford, J. J.; Gibbons, W. A.; Niccolai, N. *J. Magn. Reson.* **1982**, *47*, 522.
- (45) Shapiro, M. J.; Kolpak, M. X.; Lemke, T. L. *J. Org. Chem.* **1984**, *49*, 187.
- (46) Sanders, J. K. M.; Hunter, B. K. *Modern NMR Spectroscopy*; Oxford University Press: Oxford, 1993; p 160.

- (47) Inoue, Y.; Kuan, F.; Takahashi, Y.; Chujo, R. *Carbohydr. Res.* **1985**, *135*, C12.
- (48) Yamamoto, Y.; Onda, M.; Kitagawa, M.; Inoue, Y. *Carbohydr. Res.* **1987**, *167*, C11.
- (49) Inoue, Y.; Hoshi, H.; Sakurai, M.; Chujo, R. *J. Am. Chem. Soc.* **1985**, *107*, 2319.
- (50) Bergeron, R. J.; Channing, M. A.; Gibeily, G. J.; Pillor, D. M. *J. Am. Chem. Soc.* **1977**, *99*, 5146.
- (51) Bergeron, R.J.; Channing, M. A. *J. Am. Chem. Soc.* **1979**, *101* (10), 2511.
- (52) Harata, K.; Uekama, K.; Otagiri, M.; Hirayama, F. *Bull. Chem. Soc. Jpn.* **1982**, *55*, 3904.
- (53) Botsi, A.; Yannakopoulou, K.; Hadjoudis, E. *Magn. Reson. Chem.* **1996**, *34*, 419.
- (54) Harata, K. *Bull. Chem. Soc. Jpn.* **1977**, *50*, 1416.
- (55) Levy, G. C.; Lichter, R.L. *Nitrogen-15 Nuclear Magnetic Resonance Spectroscopy*; John Wiley & Sons: New York, 1979; p 5.
- (56) Inoue, Y.; Okuda, Y.; Miyata, Y.; Chujo, R. *Carbohydr. Res.* **1984**, *125*, 65.
- (57) Reichardt, C. *Solvents and Solvent Effects in Organic Chemistry*; VCH Publishers, Inc.: New York, 1988; p 5.

- (58) Ando, I.; Webb, G. A. *Org. Magn. Reson.* **1981**, *15*, 111.
- (59) Inoue, Y.; Furuki, T.; Hosokawa, F.; Sakurai, M.; Chujo, R. *J. Am. Chem. Soc.* **1993**, *115*, 2903.
- (60) Sakurai, M.; Hoshi, H.; Inoue, Y.; Chujo, R. *Chemical Physics Letters* **1989**, *163* (2,3), 217.
- (61) Barfield, M.; Karplus, M. *J. Am. Chem. Soc.* **1969**, *91*, 1.
- (62) Neuhaus, D.; Williamson, M. *The Nuclear Overhauser Effect*; VCH Publishers, Inc.: New York, 1989; p 141.
- (63) Yamamoto, Y.; Onda, M.; Takahashi, Y.; Inoue, Y.; Chujo, R. *Carbohydr. Res.* **1988**, *182*, 41.
- (64) Lehn, J. M.; Boger, J.; Corcoran, R. J. *Helvetica Chimica Acta* **1978**, *61*, 2190.
- (65) Tanimoto, T.; Kubota, Y.; Nakanishi, N.; Koizumi, K. *Chem. Pharm. Bull.* **1990**, *38*(2) . 318.
- (66) Casu, B.; Reggiani, M.; Gallo, G. G.; Vigevani, A. *Tetrahedron* **1968**, *24*, 803.
- (67) Gaude, D.; Le Goaller, R.; Pierre, J. L. *Synthetic Communications* **1986**, *16*(1), 63.
- (68) Gruenhut, N. S.; Cushing, M. L.; Caeser, G. V. *J. Am. Chem. Soc.* **1948**, *70*, 424.
- (69) Freudenberg, K.; Cramer, F. *Chem. Ber.* **1950**, *83*, 296.

- (70) Liebowitz, J.; Silmann, S. H.; *Chem. Ber.* **1925**, 58, 1889.
- (71) Dawoud, A. F.; Marawan, A. *Carbohydr. Res.* **1973**, 26, 65.
- (72) Bulusu, S.; Axenrod, T.; Ling, B.; Yuan, L. *Magn. Reson. Chem.* **1989**, 29, 168.
- (73) Narasimhan, S.; Srinivasan, S. K.; Venkatasubramanian, N. K. *Magn. Reson. Chem.* **1987**, 25, 91.
- (74) Axenrod, T.; Liang, B.; Bulusu, S. *Magn. Reson. Chem.* **1989**, 27, 925.

# IMAGE EVALUATION TEST TARGET (QA-3)



APPLIED IMAGE, Inc  
1653 East Main Street  
Rochester, NY 14609 USA  
Phone: 716/482-0300  
Fax: 716/288-5989

© 1993, Applied Image, Inc.. All Rights Reserved

